Reduced continental weathering and marine calcification linked to late Neogene decline in atmospheric CO_2

Weimin Si [a, b, *], Yair Rosenthal [a, b]

a) Department of Earth and Planetary Sciences, Rutgers University

b) Department of Marine and Coastal Sciences, Rutgers University

- Corresponding author now at Department of Earth, Environmental, and Planetary Sciences, Brown University

Abstract: 188 words

Main Text: 2921 words

The globally-averaged Calcite Compensation Depth has deepened by several hundred meters in the last 15 Myr. This deepening has previously been interpreted to reflect increased alkalinity supply to the ocean driven by enhanced continental weathering due to the Himalayan orogeny during the late Neogene. Here we examine Mass Accumulation Rates of the main marine calcifying groups and show that global accumulation of pelagic carbonates has decreased from the late Miocene to the late Pleistocene even though $CaCO_3$ preservation has improved, suggesting a decrease in weathering alkalinity input to the ocean, thus opposing expectations from the Himalayan uplift hypothesis. Instead, changes in relative contributions of coccoliths and planktonic foraminifera to the pelagic carbonates in relative shallow sites, where dissolution has not taken its toll, suggest that coccolith production in the euphotic zone decreased concomitantly with the reduction in weathering alkalinity inputs as registered by the decline in pelagic carbonate accumulation. Our work highlights a new mechanism whereby in addition to deep sea dissolution, changes in marine calcification acted to modulate carbonate compensation in response to reduced weathering linked to the late Neogene cooling and decline in atmospheric pCO_2.

Earth's climate in the Neogene (~23-2.58 Ma) is characterized by successive cooling steps that culminated in Quaternary glaciations [1]. The origin of this long-term cooling, however, remains debatable. On geological timescales, atmospheric pCO_2, considered as the prime climate forcing, is regulated through the balance between volcanic/metamorphic outgassing, silicate weathering and organic matter burial [2]. In the Neogene, seafloor spreading rates and, by inference, outgassing rates appear to have been relatively constant [3], leading to the corollary that Neogene decrease in pCO_2 and climate cooling may have been primarily driven by enhanced weathering; it has been argued that the Neogene uplift of the Himalayas may have enhanced rock weathering due to increased exposure of weatherable rock surfaces [4, 5]. The weathering hypothesis (aka Raymo's hypothesis), however, is controversial because it argues that weathering can act as a forcing, rather than a stabilizing feedback of the Earth's thermostat [2, 6, 7]. The alternate hypothesis (aka Berner's hypothesis), relates high weathering fluxes to the impact of high atmospheric pCO_2 and warm surface temperatures, which provides a necessary feedback to stabilize climate [2]. Accordingly, Neogene cooling should have resulted in reduced, rather than enhanced, continental weathering.

In a steady-state ocean, weathering fluxes of dissolved solutes to the sea must be balanced by output fluxes. With regard to the ocean's carbonate alkalinity budget, the balance between riverine alkalinity input and $CaCO_3$ burial is achieved through $CaCO_3$ dissolution. Pelagic calcifying species, planktonic foraminifera and coccolithophores, produce today ~50 Tmol/yr carbonates in the upper ocean [8, 9, 10], consuming ~3 times the alkalinity that is made available to the ocean from rivers (~33 T eq/yr [11]). To restore ocean's alkalinity budget, dissolution will take place in the deep sea. The balancing process is arguably manifested in the Calcite Compensation

Depth (CCD) [12], below which seawater is sufficiently undersaturated to dissolve all $CaCO_3$. Raymo's hypothesis [4] and Berner's hypothesis [2] have different predictions as to the change in global $CaCO_3$ burial through the Neogene. Berner's hypothesis predicts high alkalinity and burial fluxes in the early Neogene decreasing to the present, whereas Raymo's hypothesis predicts the opposite. These trends should, in principle, be reflected in the CCD.

For the last 15 Myr, the globally-averaged CCD has deepened by ~500 m [13]. This deepening has been interpreted as increased carbonate burial fluxes in response to higher riverine alkalinity input as the result of enhanced chemical weathering from mountain building [4, 5]. However, the CCD-based interpretation relies critically on the assumption of constant carbonate production. Instead, we propose that environmentally-driven changes in the production of marine calcifiers have also played an important role in the long-term calcite compensation thereby modulating the pelagic carbonate burial rate, supporting recent model results suggesting that the CCD alone is insufficient to constrain neither the dissolution nor the accumulation of pelagic carbonate [14]. Therefore, instead of reconstructing the paleo-CCD, as was done previously, we reconstruct late Neogene (0-15 Ma) pelagic carbonate production and dissolution by documenting Mass Accumulation Rates of carbonate sediment (MARc) and its main producers, coccolithophores (MAR-coccolith) and planktonic foraminifera (MAR-foram) from various ocean basins and depths (Figure 1), particularly along depth transects where the effects of production and dissolution can be distinguished. Because coccolithophores and foraminifera are different in terms of their ecology (autotrophic vs heterotrophic) and calcification processes, distinguishing between the history of MAR-coccolith and MAR-foram, is critical to an improved understanding of long-term carbonate cycle changes. Applying this approach to five deep sea cores selected

above the lysocline (<2.6 km depth), it has been suggested that decreasing pelagic carbonate burial rates over the late Neogene was likely driven by decreasing MAR-coccolith possibly in response to a decline in continental weathering [15]. Here we extend the study to >30 sites to test the globality of the suggested changes and provide stronger constraints on its causes and implications to the carbon cycle.

Changes in MARc over the past 15 Myr

Among MARc records we investigated, many of them show a decreasing trend following the late Miocene productivity pulse to the late Pleistocene, consistent with previous studies [15, 16]. To summarize the trends, we average the MARc in three approximately evenly spaced intervals, i.e. Pleistocene, 0-2.5 Ma, Late Miocene, 5.3-7.5 Ma, and Middle Miocene 11.5-13.5 Ma (Figure 2, Table S3). Multi-myr averages are used because they presumably reflect long-term steady states and also minimize age model uncertainties. Because a range of processes can affect local carbonate accumulation, temporal variations of MARc from the Middle-Late Miocene to the Pleistocene are expected to be spatially heterogeneous. Two global features, however, stand out.

First, MARc have decreased significantly in relatively shallow sites (< 3000 meters below sea level, mbsl) but show little variations in deeper sites. This is best illustrated by two depth transects in the equatorial Pacific (Figures 2a-b). In the western Equatorial Pacific, MARc of the shallowest site (Site 806) decreased from >4 g/cm^2 kyr in the Miocene to ~1.7 g/cm^2 kyr in the Pleistocene. Concomitantly, MARc in the shallow central equatorial Pacific decreased from ~2-3 g/cm^2 kyr to ~1 g/cm^2 kyr. In contrast, MARc of both regions show little variations at ~4000 mbsl, consistent with a previous reconstruction suggesting relatively constant CCD in the Pacific

since 15 Ma [17]. Secondly, large decreases in MARc have also occurred in other regions where today's carbonate production and burial potentials are high (Figure 2c-d), such as the southwest Pacific and North Atlantic [9]. In the North Atlantic, MARc of Site 982 (1134 mbsl) decreased from >5 to ~1.5 g/cm^2 kyr. Similar magnitude of decreases is also seen at Site 590 at 1300 mbsl in the western Pacific.

The temporal pattern of decreasing MARc becomes less apparent in the equatorial Atlantic and South Atlantic. At Site 925, MARc have remained approximately constant, decreasing only by ~1 g/cm^2 kyr in the Late Pleistocene (Figure 3, Fig. S1). In the South Atlantic, MARc of Site 1264 has a temporal pattern (Fig. S1) that is more similar to nearby continental margin Site 1085 [18], high in the Late Miocene, but low in the Pleistocene as well as in the Middle Miocene. In the deep South Atlantic, MARc of Sites 928 and 1266 show some increases over time, consistent with previous CCD reconstruction of a deepening toward the Pleistocene. Higher Pleistocene MARc at Site 1266, however, may be partially due to winnowing and redeposition (Supporting Information). The equatorial Indian Ocean exhibits the lowest pelagic MARc (<1.5 g/cm^2 kyr) and the smallest variations (<0.5 g/cm^2 kyr) of all basins throughout the late Neogene (Fig. S1).

Dissolution of deep-sea carbonate during the last 15 Myr

Decreases in MARc in the Pacific and the Atlantic can be due to either increased dissolution and/or decreased production. We examine the carbonate preservation along a depth transect on the Ontong-Java Plateau in the western equatorial Pacific (Sites 806-804) where the deep water likely represents the mean ocean. The $CaCO_3$ content at this transect is ~90% between ~15-6 Ma decreasing to ~80% during the last 6 Myr (Figure 3a). Given relatively constant non-carbonate

MAR (~0.2-0.4 g/cm$_2$ kyr, Fig. S1), this decrease may be interpreted as increased dissolution in the past 6 Myr, particularly at deepest Site 804 (3800 mbsl).

The preservation of the planktonic foraminifera, however, indicates the opposite. We introduce a new coccolith-free size dissolution index (weight ratio of >60 μm/>20 μm, henceforth CF-size index) to qualitatively evaluate the preservation of planktonic foraminifera (Supporting Information). Compared to conventional dissolution index based on coarse fraction content [19, 20, 21, 22], the CF-size index only examines the foraminiferal fraction (>20 μm) by excluding the coccolith fraction (<20 μm) that may potentially bias dissolution estimates due to changes in coccolith productivity. Accordingly, high (low) CF-size index values indicate high (low) degree of foraminiferal shell preservation. From the depth transect of Sites 806-804, the CF-size indices show general increasing trends throughout the past ~14 Myr (Figure 3b), which, in contrast with the interpretation from the %$CaCO_3$, suggests improved preservation over time. The trend of progressively enhanced foraminiferal preservation is only interrupted at ~10-8 Ma when a minimum values indicate that about half of the foraminiferal shells in the oozes are in the form of fine fragments (20-60 μm). These changes in preservation can also be visually recognized under the light microscope, which shows increasing abundance of whole-shell foraminifera over time (Fig. S7). We also note that the CF-size index can be affected by other processes, including foraminiferal evolution and burial diagenesis, although these processes do not seem to compromise our main conclusion (Supporting Information).

MAR-foram from the depth transect further support higher dissolution in the Middle-Late Miocene. In the Pleistocene, average MAR-foram are ~0.45 and ~0.27 g/cm$_2$ kyr at the shallow

Site 806 and deeper Site 803, respectively, suggesting minimal dissolution between 2500-3400 mbsl. This estimate is close to Holocene estimates based on radiocarbon ages of core-top materials, which suggests ~0.4 g/cm$_2$ kyr foraminiferal dissolution over this depth interval (Table S5). During 11.5-13.5 Ma, however, the MAR-foram were ~1.5 g/cm$_2$ kyr at Sites 806 and ~0.25 g/cm$_2$ kyr at Site 803, respectively, indicating more than 1 g/cm$_2$ kyr of planktonic foraminifera had dissolved over the same depth interval.

Away from the equatorial Pacific, we also find overall increases in the CF-size index in the southwest Pacific, tropical Indian Ocean, South Atlantic, and equatorial Atlantic, even though the timing and patterns vary from site to site (Fig. S8). Taken together, our data suggest that the deep sea has become more saturated with respect to carbonate since the Middle Miocene.

Linking dissolution to reduced calcification

When carbonate production is constant, the correlation between dissolution and carbonate accumulation is straightforward. More dissolution implies less burial, and vice-versa (Fig. S9a). Carbonate dissolution can also be affected by the thickness of the transition zone, which is defined as the depth interval between the calcite saturation horizon and the CCD. If the transition zone becomes thicker, dissolution increases even though the CCD remains constant (Fig. S9b). Variations in the thickness of the transition zone given constant CCD, therefore, have been invoked to explain changes in carbonate burial [17, 23].

Apparently paradoxical evidence of decreasing carbonate accumulation in a progressively more saturated ocean suggest that decreased pelagic carbonate production rather than enhanced

dissolution is responsible for reduced carbonate accumulation during the late Neogene. In the modern ocean, sediment traps indicate that the median of carbonate production in mid- and low-latitudes (60°S-60°N) is ~1.2 g/cm^2 kyr [24] (Fig. S10), a value close to Pleistocene MARc of relatively shallow sites where the dissolution effect is limited (Figure 4). In contrast, MARc from the same set of sites suggest much higher carbonate production in the Middle-Late Miocene.

Because pelagic carbonates are mainly precipitated from coccolithophores and planktonic foraminifera, we calculated MAR-foram and MAR-coccolith to investigate their relative contributions to higher Miocene MARc (Figure 4, Fig. S1). The calculation shows that MAR-foram remained nearly constant over time, whereas MAR-coccolith has decreased significantly during the late Neogene, consistent with previous findings [15]. As foraminiferal preservation has improved during this interval, we conclude that decreasing carbonate production from coccolithophores is responsible for the decreased MARc.

Critically, changes in carbonate production result in biological compensation [14], complicating the relationships among CCD, carbonate accumulation and saturation state of seawater. For instance, although the CCD has remained relatively constant in the equatorial Pacific, dissolution close to the CCD was much stronger in the Middle-Late Miocene than in the Pleistocene (Figure 5). On the other hand, despite a thicker transition zone and stronger dissolution, carbonate burial within the transition zone was higher in the Middle-Late Miocene. Overall, it appears that enhanced coccolith production in the Miocene "outcompete" stronger dissolution at that time and resulted in higher net carbonate accumulation above the CCD.

Link between marine calcification and weathering

In a steady-state ocean, continental weathering, which is the source of alkalinity into the ocean, is largely balanced by $CaCO_3$ burial. In order to evaluate the significance of the observed decrease in MARc in terms of the ocean carbonate budget, the compensation effects due to a deeper Pleistocene CCD should also be considered. In the North Atlantic, the CCD has likely deepened from ~4 km to ~5 km from the Miocene to the Pleistocene, introducing a compensation effect on the order of ~1.2 g/cm^2 kyr (based on MARc estimates for modern ocean [9], Fig. S10). Observed decreases in MARc, however, vary from ~1-4 g/cm^2 kyr. Thus, deeper Pleistocene CCD should have only partially compensated for decreased MARc. In the equatorial Pacific, carbonate burial has most likely experienced a net decrease given its relatively constant CCD since 15 Ma [17]. A recent study suggests that CCD might have deepened by ~500 m in this region [25]. However, this deepening only introduces a small burial flux of <0.5 g/cm^2 kyr below 4 km based on modeling study [9] (Fig. S10), negligible relative to the reduced carbonate production in our records (2~3 g/cm^2 kyr). Considering the hypsometry of the ocean, we argue that Pleistocene compensation is insufficient to account for the observed large decreases in MARc from within and above the transition zone.

In addition to mid- and low-latitude pelagic oceans, MARc have also decreased in subpolar regions where coccolith oozes were replaced by diatom oozes in Pleistocene/Pliocene sediments (e.g. ODP 747, Kerguelen Plateau [26]). On continental shelves and slopes, carbonate accumulation is also believed to be higher in the Miocene due to higher sea-levels [27]. Taken together, we suggest that global carbonate burial has decreased since 15 Ma, implying that weathering alkalinity input to the ocean has also decreased as the climate cooled. Although, based on our

MARc records we cannot determine whether the decrease in alkalinity flux represents a change in continental limestone or silicate rock weathering, we note that studies of Himalayas rivers show that carbonate and silicate rocks weathering are potentially coupled [28], leading us to argue that qualitatively the late Neogene decrease in MARc suggests a decrease in the global chemical weathering flux of both rock types in contradiction with the uplift weathering hypothesis [4].

Our argument is further supported by both regional and global proxies indicating changes in chemical weathering. In the South China Sea and the Indian Ocean, chemical and mineralogical indices that have been used to monitor the intensity of chemical weathering suggest a wet climate and strong chemical weathering in the Himalayas during the Middle Miocene, followed by a long, steady decline in wetness and weathering after ~10 Ma [29]. Globally, seawater δ_7Li began to increase at ~15 Ma [30]. This increase has been interpreted as increasingly incongruent weathering that is characteristic of weathering-limited regimes. Under weathering-limited regimes, weatherable materials such as fresh rocks are in sufficient supply but weathering rates are limited by climatic factors such as temperature and precipitation [31]. Increasingly cooling climate in the late Neogene thus should have decreased chemical rock weathering, reducing the alkalinity input to the ocean. Collectively these records support our interpretation of decreased chemical weathering in a cooling climate.

Essential to our model is a link between biologic [14] and chemical compensation due to concomitant decreases in weathering fluxes and coccolith production over the course of the late Neogene. In other word, the ratio of calcite production to ingredient supply has not undergone large changes through time [32]. This covariation ultimately resulted in relative stability of the

CCD. The puzzle is — how oligotrophic calcifiers, coccolithophores, are able to "sense" the changes in continental weathering and "adjust" their carbonate production accordingly? One hypothesis is that this potential coupling may have occurred through atmospheric pCO_2 [15, 33]. In the late Neogene, decreasing pCO_2 may have become a limiting factor for photosynthesis in coccolithophores and promoted an active acquisition of cellular CO_2 through carbon concentration mechanisms (CCM) [34]. Because coccolithophores calcify within the cell, their calcification and photosynthesis machineries likely share the same cellular carbon pool. Hence, CCM may have reduced coccoliths production through the preferential allocation of cellular carbon uptake for photosynthesis over calcification [34, 35] under low pCO_2. Carbon limitation may also favor smaller coccolithophores that have higher surface/volume ratios and may have contributed to the downsizing of coccoliths [15] that is associated with the major taxonomic turnover in the Pliocene [36]. If this is the case, late Neogene MAR-coccolith would serve as a good example of how cellular-level evolution has propagated into global effects on geologic timescales.

On the other hand, weakened calcification and size reduction could not be the sole driver of weakened carbonate pump. Changes in nutrient supply likely contributed to regional differences. For instance, the persistently low late Neogene carbonate productivity in the equatorial Indian is likely associated with the absence of major upwelling in the region, whereas higher MAR-coccolith in the eastern equatorial Pacific during the Middle Miocene may be related to the higher nutrient supplies at that time[37, 38]. These observations suggest that changes in coccolith accumulation is likely productivity related. If this is the case, decreasing pCO_2 may have affected the coccolith production more indirectly through oceanographic links.

Although specific mechanisms remain yet to be investigated, we find no evidence for negative feedback between biologic calcification and more acidic/warmer ocean that is often concerned in the study of future climate changes [39]. Instead, there is apparently much more calcification in the warmer and more acidic Miocene ocean. In the late Neogene, the co-evolution of coccolithophores and continental weathering have resulted in simultaneous decreases in the carbonate production in the surface ocean and the accumulation in the deep-sea. As a result, the ocean has become less "chalky" in both the sunlit zone and the abyss as the Earth descended into an Ice-house world.

Reference

1. Zachos J, Pagani M, Sloan L, Thomas E, Billups K. Trends, rhythms, and aberrations in global climate 65 Ma to present. *Science* 2001, **292**(5517)**:** 686-693.

2. Berner RA, Lasaga AC, Garrels RM. The carbonate-silicate geochemical cycle and its effect on atmospheric carbon dioxide over the past 100 million years. *American Journal of Science* 1983, **283**(7)**:** 641-683.

3. Rowley DB. Rate of plate creation and destruction: 180 Ma to present. *Geological Society of America Bulletin* 2002, **114**(8)**:** 927-933.

4. Raymo ME, Ruddiman WF, Froelich PN. Influence of late Cenozoic mountain building on ocean geochemical cycles. *Geology* 1988, **16**(7)**:** 649-653.

5. Raymo ME. Geochemical evidence supporting TC Chamberlin's theory of glaciation. *Geology* 1991, **19**(4)**:** 344-347.

6. Berner RA, Caldeira K. The need for mass balance and feedback in the geochemical carbon cycle. *Geology* 1997, **25**(10)**:** 955-956.

7. Walker JC, Hays P, Kasting JF. A negative feedback mechanism for the long-term stabilization of Earth's surface temperature. *Journal of Geophysical Research* 1981, **86:** 9776-9782.

8. Berelson WM, Balch WM, Najjar R, Feely RA, Sabine C, Lee K. Relating estimates of CaCO3 production, export, and dissolution in the water column to measurements of CaCO3 rain into sediment traps and dissolution on the sea floor: A revised global carbonate budget. *Global Biogeochemical Cycles* 2007, **21**(1)**:** doi.org/10.1029/2006GB002803.

9. Dunne JP, Hales B, Toggweiler JR. Global calcite cycling constrained by sediment preservation controls. *Global Biogeochemical Cycles* 2012, **26**(3)**:** doi.org/10.1029/2010GB003935

10. Milliman JD. Production and Accumulation of Calcium-Carbonate in the Ocean - Budget of a Nonsteady State. *Global Biogeochemical Cycles* 1993, **7**(4)**:** 927-957.

11. Cai W, Guo X, Chen C, Dai M, Zhang L, Zhai W*, et al.* A comparative overview of weathering intensity and HCO3− flux in the world's major rivers with emphasis on the Changjiang, Huanghe, Zhujiang (Pearl) and Mississippi Rivers. *Continental Shelf Research* 2008, **28**(12)**:** 1538-1549.

12. Broecker WS. A kinetic model for the chemical composition of sea water. *Quaternary Research* 1971, **1**(2)**:** 188-207.

13. Van Andel TH. Mesozoic/Cenozoic calcite compensation depth and the global distribution of calcareous sediments. *Earth and Planetary Science Letters* 1975, **26**(2)**:** 187-194.

14. Boudreau BP, Middelburg JJ, Luo Y. The role of calcification in carbonate compensation. *Nature Geoscience* 2018, **11**(12)**:** 894.

15. Suchéras-Marx B, Henderiks J. Downsizing the pelagic carbonate factory: Impacts of calcareous nannoplankton evolution on carbonate burial over the past 17 million years. *Global and Planetary Change* 2014, **123:** 97-109.

16. Lyle M. Neogene carbonate burial in the Pacific Ocean. *Paleoceanography* 2003, **18**(3)**:** doi:10.1029/2002PA000777.

17. Pälike H, Lyle M, Nishi H, Raffi I, Ridgwell A, Gamage K*, et al.* A Cenozoic record of the equatorial Pacific carbonate compensation depth. *Nature* 2012, **488**(7413)**:** 609-614.

18. Diester-Haass L, Meyers PA, Bickert T. Carbonate crash and biogenic bloom in the late Miocene: Evidence from ODP Sites 1085, 1086, and 1087 in the Cape Basin, southeast Atlantic Ocean. *Paleoceanography* 2004, **19**(1)**:** doi.org/10.1029/2003PA000933.

19. Haug GH, Tiedemann R. Effect of the formation of the Isthmus of Panama on Atlantic Ocean thermohaline circulation. *Nature* 1998, **393**(6686)**:** 673-676.

20. Broecker WS, Clark E. CaCO3 size distribution: A paleocarbonate ion proxy? *Paleoceanography* 1999, **14**(5)**:** 596-604.

21. Chiu TC, Broecker WS. Toward better paleocarbonate ion reconstructions: New insights regarding the CaCO3 size index. *Paleoceanography* 2008, **23**(2)**:** doi.org/10.1029/2008PA001599

22. Bassinot FC, Beaufort L, Vincent E, Labeyrie LD, Rostek F, Müller PJ*, et al.* Coarse fraction fluctuations in pelagic carbonate sediments from the tropical Indian Ocean: A 1500-kyr record of carbonate dissolution. *Paleoceanography and Paleoclimatology* 1994, **9**(4)**:** 579-600.

23. Farrell JW, Prell WL. Pacific CaCO3 preservation and δ18O since 4 Ma: paleoceanic and paleoclimatic implications. *Paleoceanography* 1991, **6**(4)**:** 485-498.

24. Honjo S, Manganini SJ, Krishfield RA, Francois R. Particulate organic carbon fluxes to the ocean interior and factors controlling the biological pump: A synthesis of global sediment trap programs since 1983. *Progress in Oceanography* 2008, **76**(3)**:** 217-285.

25. Campbell SM, Moucha R, Derry LA, Raymo ME. Effects of dynamic topography on the Cenozoic carbonate compensation depth. *Geochemistry, Geophysics, Geosystems* 2018, **19**(4)**:** 1025-1034.

26. Schlich R, Wise SW, Jr., Palmer Julson AA, Aubry M-P, Berggren WA, Bitschene PR*, et al.* Site 747. *Proceedings of the Ocean Drilling Program, Initial Reports* 1989, **120:** 89-156.

27. Holland HD. Sea level, sediments and the composition of seawater. *American Journal of Science* 2005, **305**(3)**:** 220-239.

28. Tipper ET, Bickle MJ, Galy A, West AJ, Pomies C, Chapman HJ. The short term climatic sensitivity of carbonate and silicate weathering fluxes: Insight from seasonal variations in river chemistry. *Geochimica Et Cosmochimica Acta* 2006, **70**(11)**:** 2737-2754.

29. Clift PD, Hodges KV, Heslop D, Hannigan R, Van Long H, Calves G. Correlation of Himalayan exhumation rates and Asian monsoon intensity. *Nature Geoscience* 2008, **1**(12)**:** 875-880.

30. Misra S, Froelich PN. Lithium isotope history of Cenozoic seawater: changes in silicate weathering and reverse weathering. *Science* 2012, **335**(6070)**:** 818-823.

31. Kump LR, Arthur MA. Global chemical erosion during the Cenozoic: Weatherability balances the budgets. *Tectonic Uplift and Climate Change*. Springer, 1997, pp 399-426.

32. Broecker WS. A need to improve reconstructions of the fluctuations in the calcite compensation depth over the course of the Cenozoic. *Paleoceanography* 2008, **23**(1)**:** doi.org/10.1029/2007PA001456

33. Hannisdal B, Henderiks J, Liow LH. Long-term evolutionary and ecological responses of calcifying phytoplankton to changes in atmospheric CO 2. *Global Change Biology* 2012, **18**(12)**:** 3504-3516.

34. Bolton CT, Stoll HM. Late Miocene threshold response of marine algae to carbon dioxide limitation. *Nature* 2013, **500**(7464)**:** 558-562.

35. Bolton CT, Hernández-Sánchez MT, Fuertes M-A, González-Lemos S, Abrevaya L, Mendez-Vicente A*, et al.* Decrease in coccolithophore calcification and CO 2 since the middle Miocene. *Nature communications* 2016, **7:** doi: 10.1038/ncomms10284.

36. Aubry MP. A major Pliocene coccolithophore turnover: Change in morphological strategy in the photic zone. *Geol Soc Am Spec Pap* 2007, **424:** 25-51.

37. Zhang YG, Pagani M, Henderiks J, Ren HJE, Letters PS. A long history of equatorial deep-water upwelling in the Pacific Ocean. *Earth and Planetary Science Letters* 2017, **467:** 1-9.

38. Lyle M, Baldauf J. Biogenic sediment regimes in the Neogene equatorial Pacific, IODP Site U1338: Burial, production, and diatom community. *Palaeogeography, Palaeoclimatology, Palaeoecology* 2015, **433:** 106-128.

39. Boyd PW. Beyond ocean acidification. *Nature Geoscience* 2011, **4**(5)**:** 273-274.

40. Archer DE. An atlas of the distribution of calcium carbonate in sediments of the deep sea. *Global Biogeochemical Cycles* 1996, **10**(1)**:** 159-174.

41. Schlitzer R. Ocean Data View, odv.awi.de. 2018.

42. Berger WH, Bonneau MC, Parker FL. Foraminifera on the Deep-Sea Floor - Lysocline and Dissolution Rate. *Oceanologica Acta* 1982, **5**(2)**:** 249-258.

43. Baumann K-H, Böckel B, Frenz M. Coccolith contribution to South Atlantic carbonate sedimentation, in: Coccolithophores – from molecular processes to global impact, edited by: Thierstein, H. R. and Young, J. R., Springer-Verlag, 367–402, 2004., 2004.

Acknowledgement

We thank M.-P. Aubry for discussion on coccolithophorid taxonomy and evolution, D. Bord for the help with nanno-biostratigraphy and age model, X. Zhou for ICP-OES analysis. We also thank two reviewers for their constructive suggestions. This work been partially supported by NSF-OCE grant 634573 to Y.R.

Author contributions

W. S. and Y. R. conceived the idea of a global synthesis of late Neogene Mass Accumulation Rate on pelagic carbonate, foraminifera and coccoliths. W. S. performed the experiments and produced the figures. Both authors contributed to the writing of the manuscript.

Corresponding author

Correspondence and requests for materials should be addressed to W. S., weimin_si@brown.edu

Author contributions

W. S. and Y. R. conceived the idea of a global synthesis of late Neogene Mass Accumulation Rate on pelagic carbonate, foraminifera and coccoliths. W. S. performed the experiments and produced the figures. Both authors contributed to the writing of the manuscript.

Data availability

The authors declare that data supporting the findings of this study are available within the supplementary files.

FIGURE CAPTIONS

Figure 1. Deep-sea sites plotted with gridded seafloor %$CaCO_3$ [41]. We focus on open ocean sites from mid- and low-latitudes that are ecologically favored by planktonic calcifiers (coccolithophores and planktonic foraminifers) and where the seafloor is above the CCD. Pelagic settings that satisfy both criteria account for most pelagic carbonate accumulation [9, 41].

Figure 2. Changes in MARc in the Pacific and Atlantic Oceans. Black lines indicate seafloor bathymetry. a-b) equatorial Pacific depth transect. In central equatorial Pacific, plate movement and ridge subsidence can complicate the temporal trend of MARc at a single site due to the large productivity gradient across the region (Supporting Information). We therefore used a composite MARc (Figure S3) to minimize these complications; c-d) western Pacific and Atlantic latitudinal transect.

Figure 3. Improved preservation of foraminifera in the western equatorial Pacific compared to %$CaCO_3$ of bulk sediments. a) bulk %$CaCO_3$ from western Equatorial Pacific; b) CF-size index indicate improved preservation of planktonic foraminifers in the last 15 Myr.

Figure 4. Changes in MARc, MAR-foraminifers and MAR-coccolith from six relative shallow sites where dissolution is not significant.

Figure 5. Proposed conceptual model for changes in carbonate production, dissolution and accumulation in late Neogene. The model is compared to depth transect (Sites 806-804) in the western equatorial Pacific where deep-water is likely representative of the global mean. The

460 Miocene carbonate saturation horizon is estimated based on the large decreases in MARc
461 between Site 806 and 807, which suggests that significant dissolution occurred above 2.8 km.
462 Also note that dissolution occur above modern calcite saturation horizon in the Pleistocene.
463 Planktonic foraminiferal fauna analysis on core top materials (Figure S6a) [42] suggest that this is
464 likely due to the dissolution of soluble planktonic foraminifera species. The CCD is placed at
465 ~4.5 km for the last 15 Ma following an early study[18].

466 Figure 1

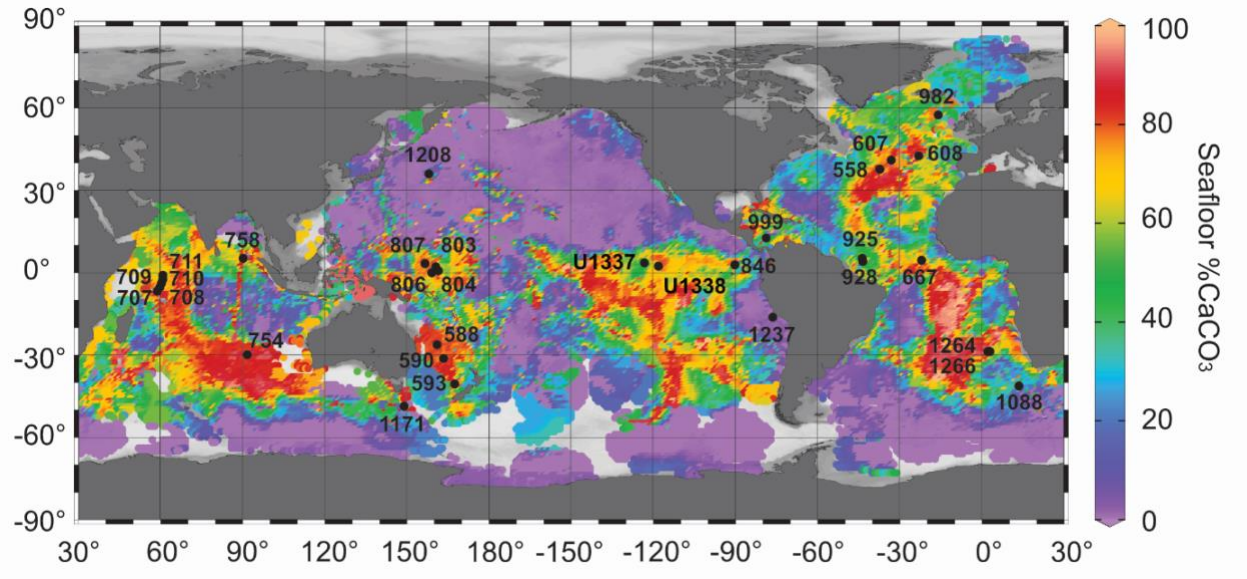

467

468 Figure 2

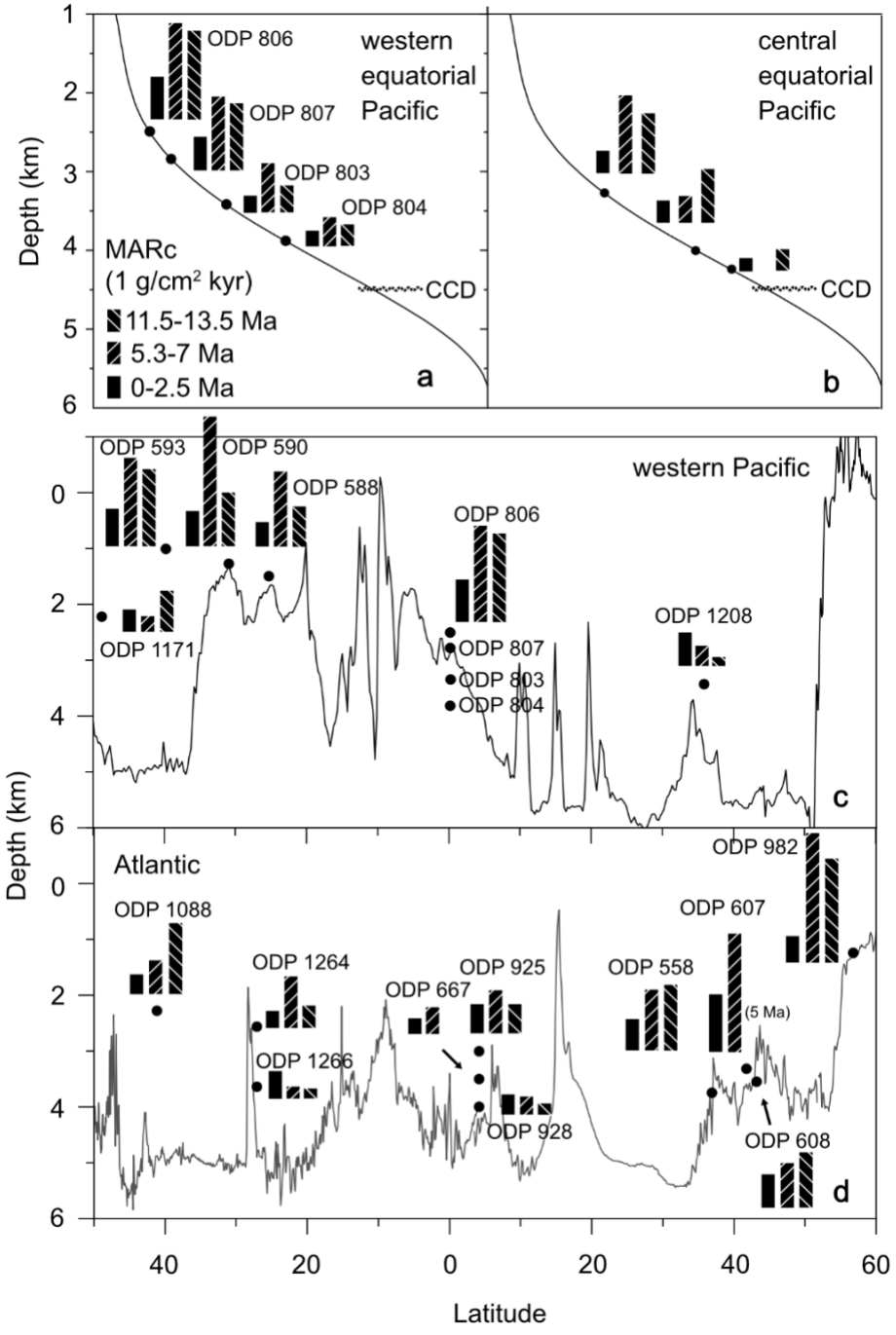

469

Figure 3.

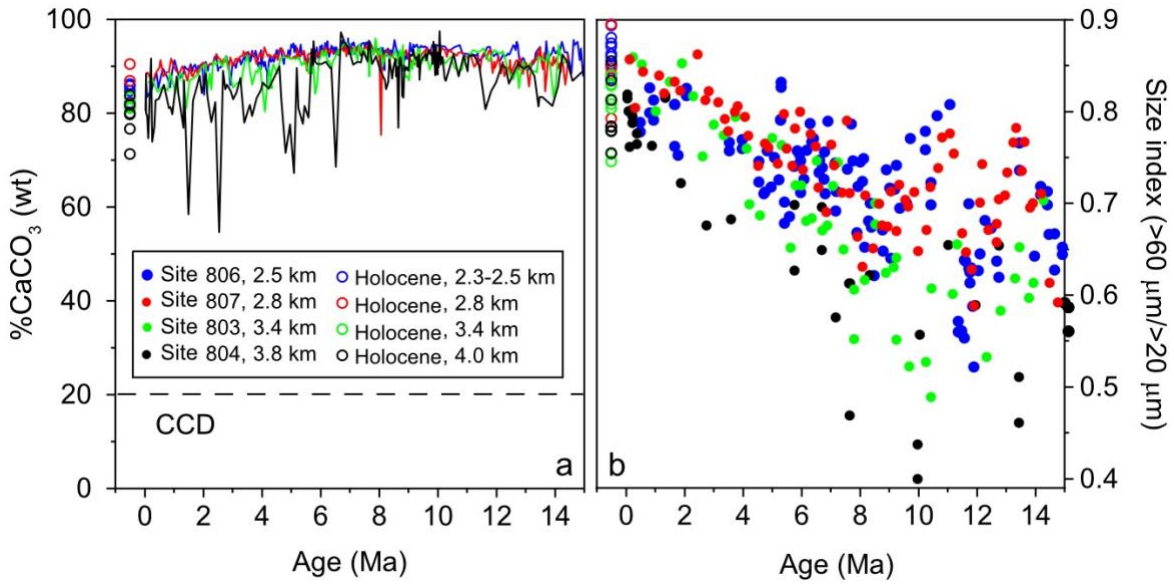
%CaCO3 (wt)
Age (Ma)
Site 806, 2.5 km
Site 807, 2.8 km
Site 803, 3.4 km
Site 804, 3.8 km
Holocene, 2.3-2.5 km
Holocene, 2.8 km
Holocene, 3.4 km
Holocene, 4.0 km
CCD
a
b
Size index (>60 µm/>20 µm)

474 Figure 4.

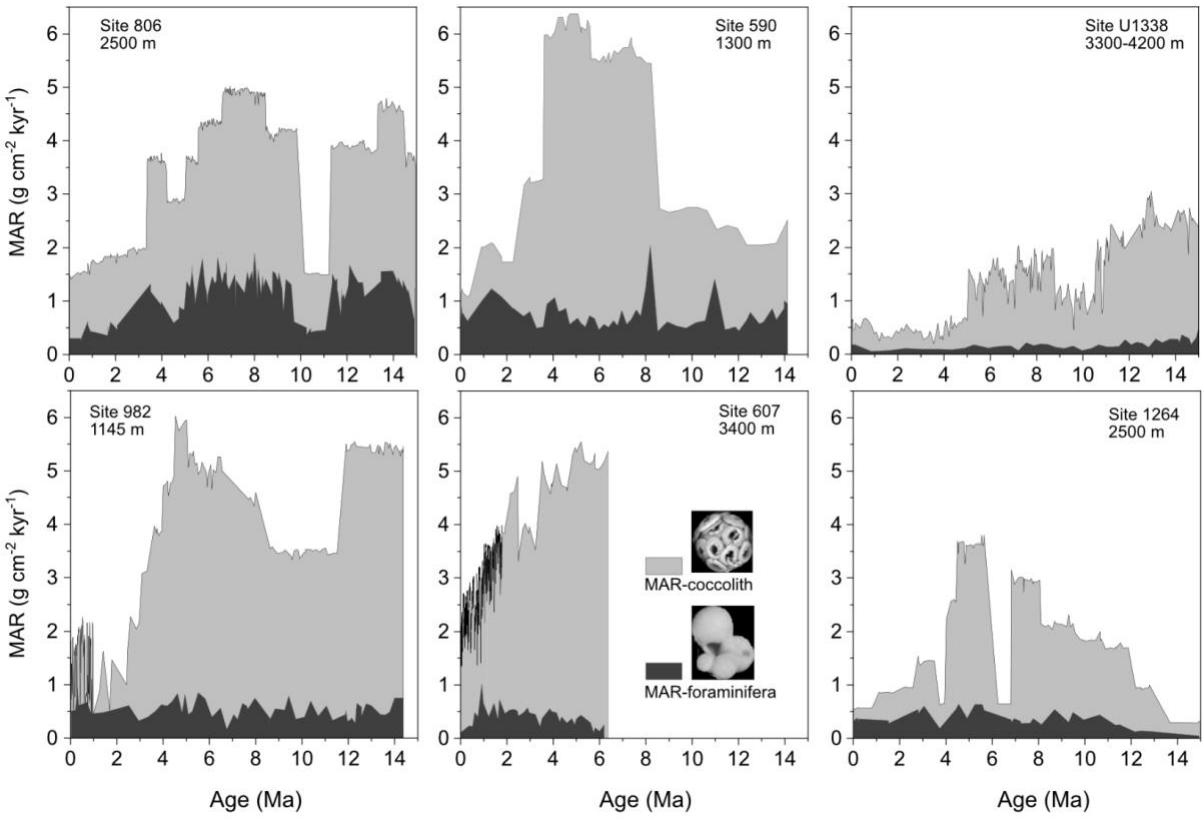

475

476

477 **Figure 5**

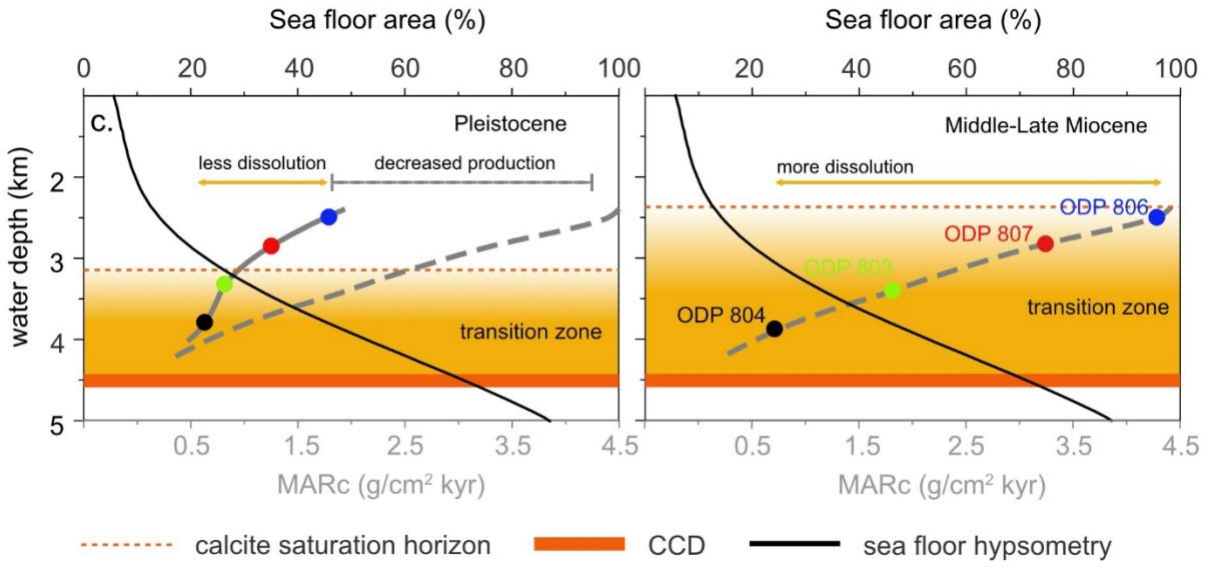

478

479

480

Supporting Information

Reduced continental weathering and marine calcification linked to late Neogene decline in atmospheric CO_2

1. Site locations and water depths
2. Composite MARc from the central Equatorial Pacific
3. Coccolith-free Size index and foraminiferal preservation
4. Potential biases in CF-size index
5. Dissolution rates of foraminifera in the Miocene, Pleistocene and Holocene sediments
6. Hypothetical scenarios of changes in carbonate production, dissolution and accumulation

	Latitude and longitude	Water depth (m)
ODP 806	0° 19.11'N, 159° 21.68' E	2521
ODP 807	3° 36.42'N, 156°37.49' E	2804
ODP 803	2° 25.98'N, 160° 32.40'E	3410
ODP 804	1° 00.28'N, 161° 35.62' E	3862
ODP 1208	36°7.6301´N, 158°12.0952´E	3346
ODP 588	26°06.7'S, 161°13.6'E	1533
ODP 590	31°10.02'S, 163°21.51'E	1299
ODP 593	40°30.47'S, 167°40.47'E	1068
ODP 1171	48°29.9960´S, 149°6.6901´E	2150
ODP U1337	3°50.009′N, 123°12.352′W;	4463
ODP U1338	2°30.469′N, 117°58.178′W	4200
ODP 1237	16°0.421´S, 76°22.685´W	3212
ODP 846	3° 5.70'S, 90° 49.08'W	3296
ODP 847	0° 11.593'N, 95° 19.22'W	3334
ODP 849	0°10.983'N, 110°31.183'W	3837
ODP 850	1°17.837'N, 110°31.283'W	3786
ODP 573	0°29.91'N, 133°18.57'W	4301
ODP 574	04°12.52'N, 133° 19.81'W	4561
ODP 982	57°31.002'N, 15°51.993'W	1134
ODP 607	41°00.068'N, 32°57.438'W	3426
ODP 608	42°50.21'N, 23°05.25'W	3526

ODP 558	37°46.2'N, 37°20.61'W	3754
ODP 667	4°34.15'N, 21°54.68'W	3539
ODP 999	12°44.639'N, 78°44.360'W	2838
ODP 925	4°12.249'N, 43°29.334'W	3053
ODP 928	5°27.320'N, 43°44.884'W	4022
ODP 1264	28°31.95´S, 2°50.73´E	2507
ODP 1266	28°32.55´S, 2°20.61´E	3798
ODP 1088	41° 8.163'S, 13° 33.770'E	2250
ODP 707	7°32.718'S, 59° 1.008'E	1553
ODP 708	05°27.35'S, 59°56.63'E	4109
ODP 709	3°54.900'S, 60°33.102'E	3040
ODP 710	04°18.7'S, 60°58.8'E	3824
ODP 711	02°44.56'S, 61°09.78'E	4429
ODP 758	5°23.049'N, 90°21.673'E	2923
ODP 754	30°56.439'S, 93°33.991'E	1074

Table S1: modern longitudes, latitudes and water depths of studied sites

Table S2

	Biostratigraphy, Paleomagnetic data, and Isotope stratigraphy	%$CaCO_3$
ODP 806	(Berger et al. 1993a, Holbourn et al. 2013, Kroenke et al. 1991a, Takayama 1993)	(Kroenke et al. 1991a)
ODP 807	(Kroenke et al. 1991d, Takayama 1993)	(Kroenke et al. 1991d)
ODP 803	(Berger et al. 1993b, Kroenke et al. 1991b)	(Kroenke et al. 1991b)
ODP 804	(Kroenke et al. 1991c, Takayama 1993)	(Kroenke et al. 1991c)
ODP 1208	(Bralower et al. 2002, Evans 2006)	(Bralower et al. 2002)
ODP 588	(Kennett et al. 1986a, Lohman 1986)	(Kennett et al. 1986a)
ODP 590	(Kennett et al. 1986b, Lohman 1986)	(Kennett et al. 1986b)
ODP 593	(Kennett et al. 1986c, Lohman 1986)	(Kennett et al. 1986c)
ODP 1171	(Exon et al. 2001)	(Exon et al. 2001)
ODP U1337	(Pälike et al. 2012)	(Pälike et al. 2012)
ODP U1338	(Pälike 2010)	(Pälike 2010)
ODP 1237	(Mix et al. 2003)	(Lopes et al. 2015)
ODP 846	(Mayer et al. 1991a, Shackleton et al. 1995)	(Mayer et al. 1991a)
ODP 847	(Farrell et al. 1995, Mayer et al. 1991b)	(Mayer et al. 1991b)
ODP 849	(Mayer et al. 1991c, Mix et al. 1995)	(Mayer et al. 1991c)
ODP 850	(Mayer et al. 1991d)	(Mayer et al. 1991d)
ODP 982	(Jansen et al. 1996, Lawrence et al. 2013)	(Jansen et al. 1996)
ODP 607	(Lisiecki and Raymo 2005, Ruddiman et al. 1987a)	(Ruddiman et al. 1987a)
ODP 608	(Ruddiman et al. 1987b)	(Ruddiman et al. 1987b)
ODP 558	(Bougault et al. 1985)	(Bougault et al. 1985)

ODP 667	(Ruddiman et al. 1988)	(Ruddiman et al. 1988)
ODP 999	(Sigurdsson et al. 1997)	(Sigurdsson et al. 1997)
ODP 925	(Curry et al. 1995a, Wilkens et al. 2017)	(Curry et al. 1995a)
ODP 928	(Curry et al. 1995b, Wilkens et al. 2017)	(Curry et al. 1995b)
ODP 1264	(Zachos et al. 2004b)	(Zachos et al. 2004b)
ODP 1266	(Zachos et al. 2004c)	(Zachos et al. 2004c)
ODP 1088	(Gersonde et al. 1999)	(Gersonde et al. 1999, Hodell et al. 2003)
ODP 758	(Peirce et al. 1989b)	(Peirce et al. 1989b)
ODP 754	(Peirce et al. 1989a)	(Littke et al. 1991, Peirce et al. 1989a)

Table S2: data source for age control points and %$CaCO_3$ data.

Table S3

	MARc (0-2.5 Ma) g cm^{-2} kyr^{-1}	SD	MARc (5.3-7 Ma) g cm^{-2} kyr^{-1}	SD	MARc (13.5-11.5) g cm^{-2} kyr^{-1}	SD
Site 1208	1.54	0.54	0.81	0.55	0.65	0.21
Site 588	1.13	0.32	3.3	0.51	1.79	0.12
Site 590	1.52	0.39	5.69	0.26	2.19	0.18
Site 593	1.59	0.28	3.78	1.41	3.63	0.08
Site 1171	1.12	0.31	0.64	0.14	1.92	0.18
Site 806	1.71	0.15	4.35	0.41	4	0.26
Site 807	1.27	0.18	3.19	0.19	3.3	0.26
Site 803	0.85	0.2	2.23	0.43	1.65	0.45
Site 804	0.64	0.09	0.8	0.3	0.75	0.03
U1337	0.19	0.18	0.47	0.31	2.46	0.57
U1338	0.49	0.12	1.4	0.23	2.46	0.31
Site 1237	0.23	0.2	2.17	0.15	1.1	0.12
Site 846	1.01	0.38	1.64	1.07	1.24	0.16
Site 982	1.45	0.54	5	0.22	5.32	0.46
Site 608	1.31	0.44	1.69	0.67	2.52	0.06
Site 607	2.57	0.63	5.31	0.16		
Site 558	1.41	0.26	2.71	0.06	3.034	0.3
Site 999	1.45	0.27	1.24	0.31	0.94	0.34
Site 667	0.71	0.18	1.31	0.22		
Site 925	1.3	0.48	1.97	0.39	1.32	0.23
Site 928	0.92	0.41	0.88	0.41	0.52	0.22
Site 1264	0.84	0.13	2.74	1.23	1.08	0.53
Site 1266	1.19	0.18	0.54	0.003	0.49	0.17
Site 1088	0.88	0.09	1.47	0.32	3.14	1.19

Site 758	0.67	0.07	0.96	0.13	0.3	0.03
Site 754	0.32	0.07	0.46	0.04	0.79	0.01

Table S3. Summary of MARc for selected time intervals in Figure 2. Note that despite $\%CaCO_3$ are available at high resolution, LSRs and MAR-bulk can only be calculated at a much lower resolution. Therefore, the calculated standard deviations (SD) here do not fully reflect the variability of the carbonate accumulation. It only reflects the variability of %CaCO3 given the age model. To prevent false impression that the MARc variations are also known at the same resolution of $\%CaCO_3$ data, the standard deviations calculated here are not reported in Figure 2.

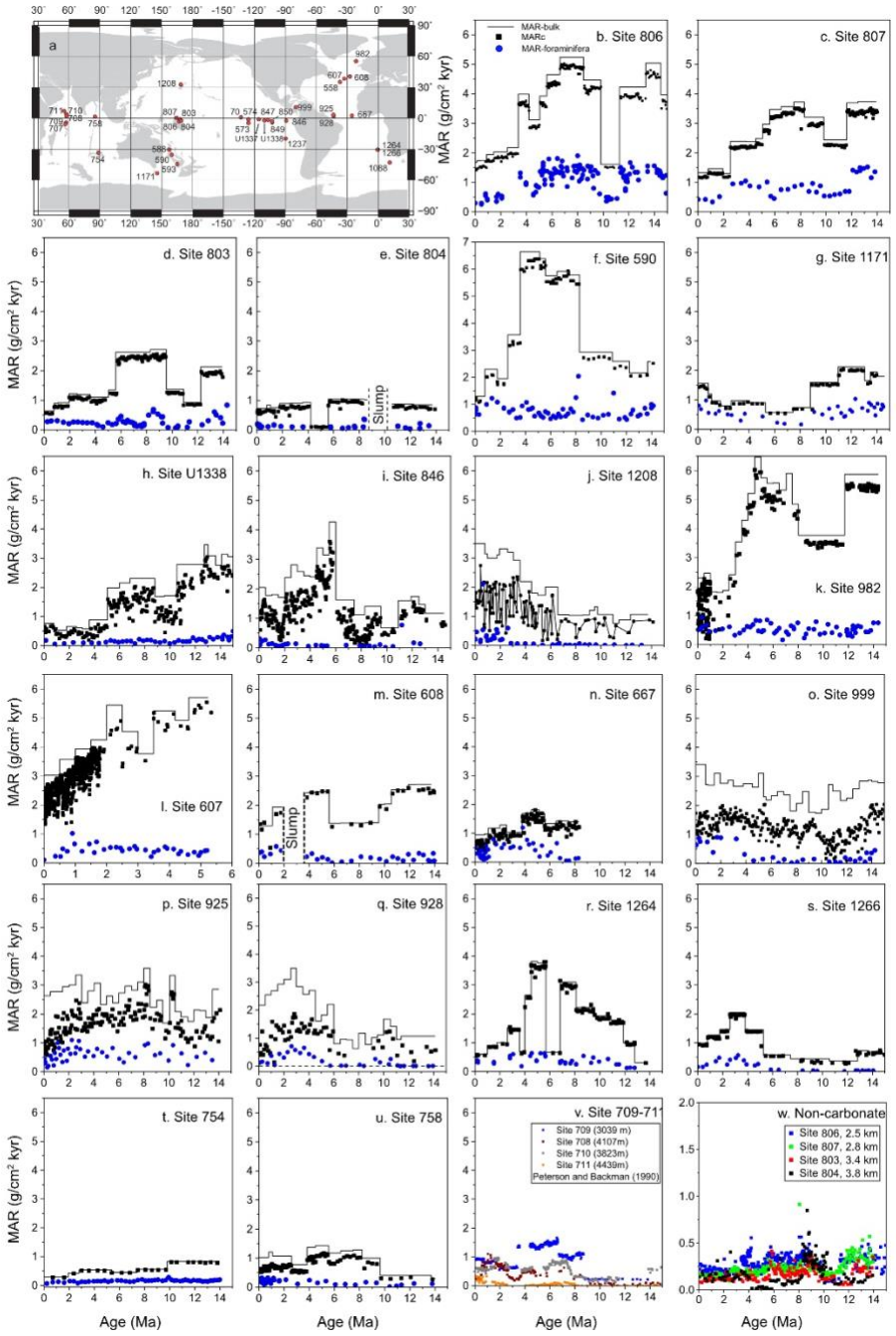

506

507 **Figure S1. (a)** Locations of sites examined for MARc. Paleo-latitude and geographic

508 reconstruction (13.5 Ma) were generated from http://www.odsn.de/; **Figure S1 (b-u).** MAR of

509 bulk samples (solid line), MARc (black squares) and MAR-foraminifera (blue dots) from the

510 Pacific (Figure S2b-j), Atlantic (Figure S2k-s), and Indian Ocean (Figure S2t-v). MARc of the

511 western equatorial Indian Ocean are from (Peterson and Backman 1990) (Figure S2v). Although

512 the dataset includes Site 707-711, the shallowest Site 707 was not considered here. Carbonate
513 content of this site is particularly low, possibly due to strong dissolution associated with local
514 circulation effect (Peterson and Backman 1990). **Note** that 1) sedimentation rates were
515 particularly high between ~8-10 Ma at Site 804. This anomalous MARc (~4 g/cm$_2$ kyr) of the
516 lower Upper Miocene section at Site 804 is especially striking when compared to more normal
517 sedimentation rates. The presence of turbidites was noted in the core descriptions (Kroenke et al.
518 1991c), suggesting redeposition during this time interval (Berger et al. 1993b); 2) Similarly,
519 sedimentation rate was particularly high at ODP 608 between 2.5 and 4 Ma. Visual observation
520 of the core photos suggests numerous slumps during the deposition of this interval. Similarly,
521 slumps occurred in cores 15 to 18 in ODP 667. Therefore, MAR was not calculated for
522 sediments older than 8 Ma at this site. 3) Other processes such as winnowing may have also
523 affected local MARc. At Walvis Ridge, MARc at 3.8 km (ODP 1266) become strangely higher
524 than that of 2.5 km (ODP 1264) in the Pleistocene. Although both sites have similar MAR-
525 foraminifera (~0.34 g/cm$_2$ kyr), MAR-coccolith at 3.7 km are much higher than at 2.5 km (0.85
526 vs 0.33 g/cm$_2$ kyr), suggesting that fine particles (coccoliths) have been moved downslope and
527 re-deposited at depth by bottom current. **Figure S1 (w)**. Mass Accumulation Rates of non-
528 carbonate (MAR-noncarb) from western Equatorial Pacific depth transect Sites 806-804.
529
530 **1. Site locations and water depths**
531 Site locations and water depths are listed in Table S1. Miocene paleolatitudes of studied sites
532 were plotted in Figure S1a. For most sites, changes in paleo-depth are small. For instance, ODP
533 1264 and 1266 from Walvis Ridge have potentially deepened by ~300 m since the Middle
534 Miocene (Zachos et al. 2004a). This deepening had only minor effects on dissolution and

535 therefore does not compromise our discussion. However, this is not the case for sites from the
536 eastern Equatorial Pacific where significant changes in latitude and depth have occurred. For
537 instance, ODP U1338 has potentially deepened by 800 m and this deepening may have
538 significantly affected the carbonate preservation (see discussion below).
539
540 **2. Composite MARc from the central Equatorial Pacific**
541 Sediment trap data show that there is a sharp productivity gradient across the equator in the
542 central Equatorial Pacific (Honjo et al. 1995). Productivity is high at the equator but decreases
543 significantly a few degrees off it (Figure S2a). Moreover, carbonate dissolution increases with
544 water depth. As a result of changes in productivity and dissolution over depths and latitudes,
545 MARc show large spatial variations in the eastern Equatorial Pacific (Figure S2b).
546
547 Over the last 15 Myr, sites in the eastern Equatorial Pacific have experienced large changes in
548 paleodepths as well as paleo-latitudes (Figure S2c). Plate movement and ridge subsidence may
549 have complicated the MARc history of a single site. For instance, changes in MARc from Site
550 U1338 (Figure S1h) cannot be simply explained either as changes in either productivity or
551 dissolution. In order to better constrain changes in MARc in this region, we have reconstructed a
552 composite MARc (Figure S3) for the selected time interval.
553

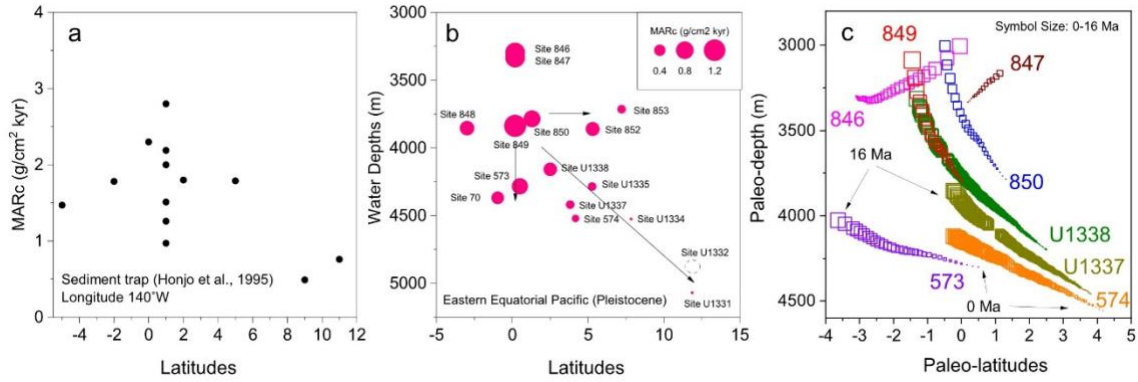

554

555 **Figure S2**. (a) sediment trap showing latitudinal variations with decreasing fluxes off the equator
556 in the eastern Equatorial Pacific; (b) Pleistocene MARc. Age model are based on paleomagnetic
557 and biostratigraphy data from ODP initial report. MARc of Site 70, 573 and 574 data are from
558 (Lyle 2003). MARc of Sites U1331, U1332, U1334, U1335 and U1337 are from (Pälike et al.
559 2012); (c) Changes in paleo-latitude and paleodepth of selected sites in the eastern Equatorial
560 Pacific. Data are from (Lyle 2003, Pälike et al. 2012).

561

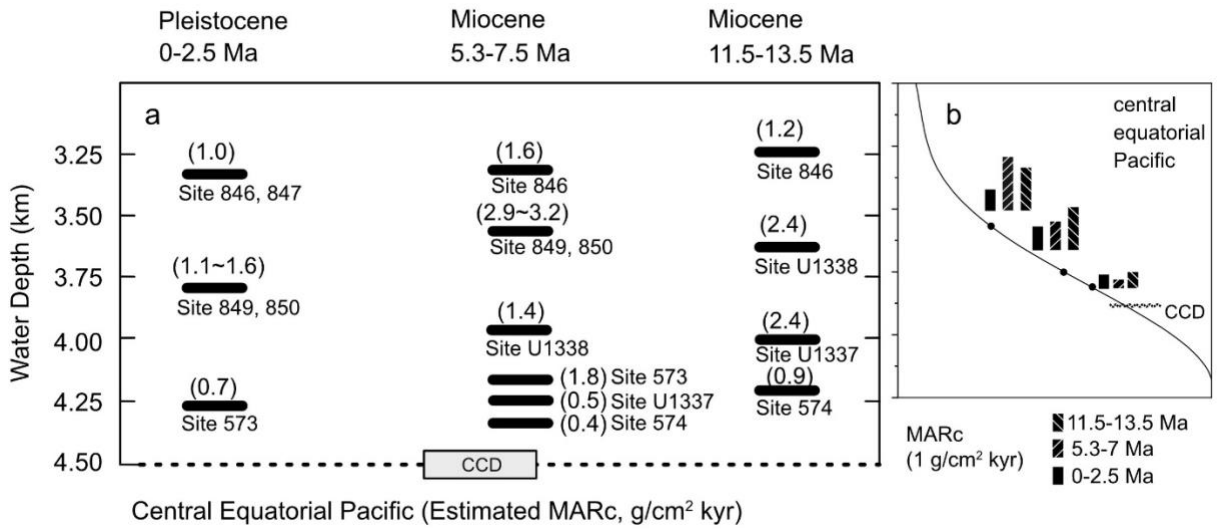

562

563 **Figure S3.** (a) sites selected for constructing composite MARc for each time interval. Numbers
564 in parentheses are estimated MARc; (b) Composite MARc of central equatorial Pacific.

565

566 **3. Coccolith-free Size index and planktonic foraminiferal preservation**

567 A simple and efficient method to evaluate the dissolution of deepsea carbonate is to measure the
568 weight ratio of coarse fraction (>60 μm/bulk carbonate) (Bickert et al. 1997, Broecker et al.
569 1999b, Haug and Tiedemann 1998, Sexton and Barker 2012). Because coccoliths are generally
570 more robust to dissolution (Beaufort et al. 2007, Hassenkam et al. 2011, Honjo and Erez 1978,
571 Roth and Berger 1975) than planktonic foraminifera, percent of coarse fraction can indicate the
572 preferential loss of foraminifera test relative to coccoliths as the dissolution proceeds. This
573 method is easy to apply and requires no tedious microscopic work. However, it implicitly
574 assumes that the ratio of planktonic foraminifera and coccoliths in the calcite rain is constant
575 (Chiu and Broecker 2008), which may not be true in the geologic past.

576

577 To overcome the complication of temporal changes in the ratio of planktonic foraminifera and
578 coccoliths in the initial carbonate rain, a better approach is to examine the preservation of the
579 planktonic foraminifera only. To this end, we first remove the coccolith fraction with a 20 μm
580 sieve. Because Cenozoic coccoliths have a dimension of <20 μm (with a few exceptions of
581 Paleogene Reticulofenestra and Coccolithus), this step can effectively separate the coccoliths
582 from foraminiferal shells. In the fraction of >20 μm, we measure the coccolith free size index
583 (CF-size index), the weight ratio of >60 μm/>20 μm. The idea is that during the dissolution,
584 planktonic foraminiferal tests are thinned/weakened and break down into small fragments,
585 moving materials from the coarse fraction (>60 μm) into finer fractions (20-60 μm) (Figure S4).
586 As dissolution proceeds, CF-size index decreases.

587

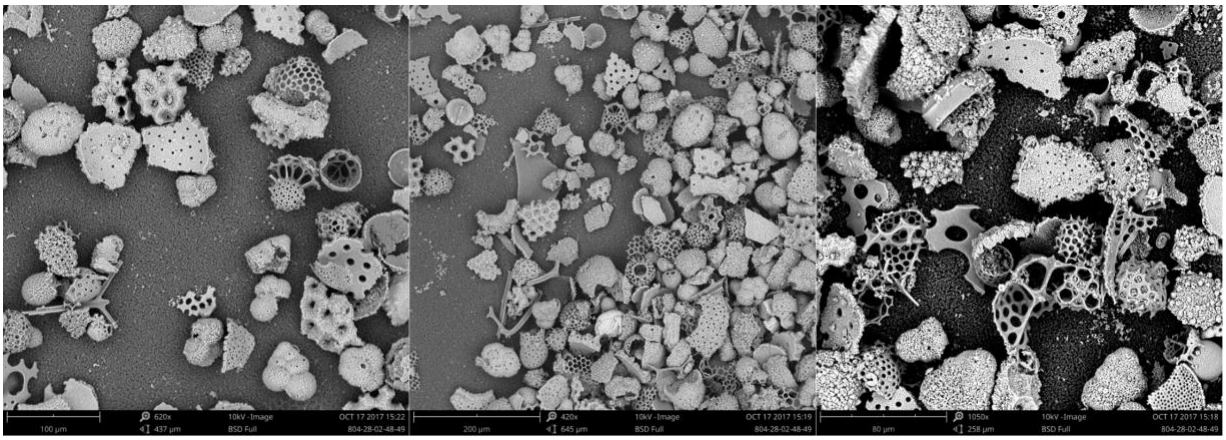

588

589 **Figure S4.** Planktonic foraminiferal fragments in the 20-60 μm (Site 804/28/02/48-49cm). SEM photos
590 are taken through a Phenom ProX Desktop SEM at Department of Marine and Coastal Sciences, Rutgers
591 University.

592

593 We first tested this method with core top samples collected along a Ontong-Java depth transect
594 in order to prove its effectiveness. We then applied it to downcore sediments of the last 15 Myr.

595

596 **3.1 Core top calibration of coccolith-free size index**

597 Samples from Ontong-Java Plateau were collected by Wood Hole Oceanographic Institution. We
598 sampled from coretop (1-5 cm) down to ~15 cm at 10 different water depths (Table S4) to
599 capture the late Holocene records (~10,000 years) based on ^{14}C age model of (Broecker and
600 Clark 1999, Broecker et al. 1999b).

601

602 Depth, coarse content (>60 μm/Total Carbonate) and CF-size index (>60 μm/>20 μm) are plotted
603 in Figure S5. Both indicators decrease with increasing water depths, suggesting decreasing
604 coarse fraction (>60 μm) with increasing undersaturation (Figure S6b). Because the initial
605 composition of carbonate rain unlikely has changed significantly over the last 8000-10,000 years

606 in the Western Equatorial Pacific, both indicators should be controlled only by the dissolution
607 and fragmentation of planktonic foraminifera.
608
609 Using the ^{14}C age measured from the same cores, Broecker et al. (1999) estimated the averaged
610 Mass Accumulation Rates (MAR) of the upper 20 cm of these cores (Table S4). We convert
611 them into the MAR-foraminifera and MAR-coccoliths based on the weight percent of <20 μm
612 (coccoliths) and >20 μm (forams) fractions. We find that the MAR-foraminifera decreases from
613 0.98 g/cm^2 kyr at 2.3 km to 0.2 g/cm^2 kyr at 4.04 km, suggesting ~80% of the planktonic
614 foraminifera have dissolved over this depth interval. Much of the dissolution, indeed, occur
615 between 2.31 and 3.39 km where our size index began to decrease (Figure S5b) and the seawater
616 changes from slightly oversaturated to undersaturated (Figure 6b). A quick inspection of the >60
617 μm fraction under microscope show significant changes in the fauna composition (Figure S6c)
618 characterized by the disappearance of more soluble species such as pink *Globigerinoides ruber*
619 and the enrichment of dissolution resistant species such as *Pulleniatina obliquloculata*.
620
621 Another feature of the CF-size index (>60 μm/>20 μm) is the temporal trend in late Holocene in
622 deeper sites. Above 3500 m, the downcore changes in the >60 μm/>20 μm appear to be small
623 (Figure S5b), suggesting that the preservation of foraminifera has not changed significantly over
624 the last 8000 years. However, the preservations of foraminifera are significantly better 8000-
625 10,000 years ago than the core top at 4.5 km water depth (Figure S5b, the size of symbols
626 indicating sampling depth). Discussion on Paleoceanographic significance of this event is
627 beyond the scope of this study. readers can refer the following studies (Broecker and Clark 2007,
628 Broecker et al. 1999b, Keir and Berger 1985). Because our measurements are consistent with

629 other dissolution indicators and suggest decreased preservation in the Pacific in the last 8000-
630 10,000 years, it further validates CF-size index as an efficient dissolution indicator.
631

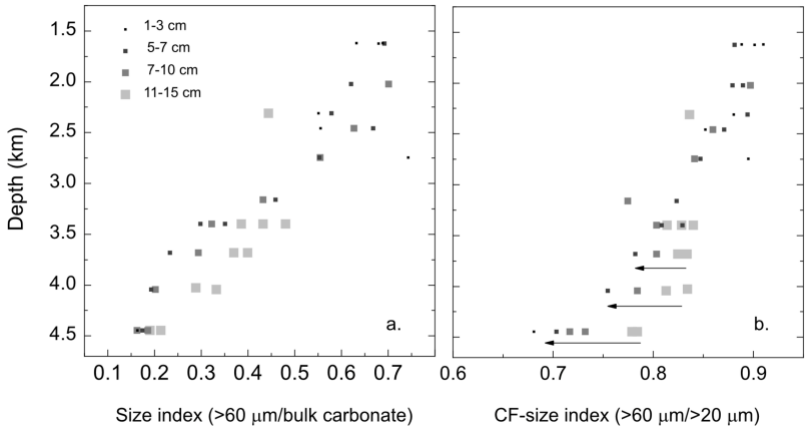

632

633 **Figure S5.** (a) depth profiles of coarse content (>60 μm/Total Carbonate); (b) CF-size index
634 (>60 μm/>20 μm);
635

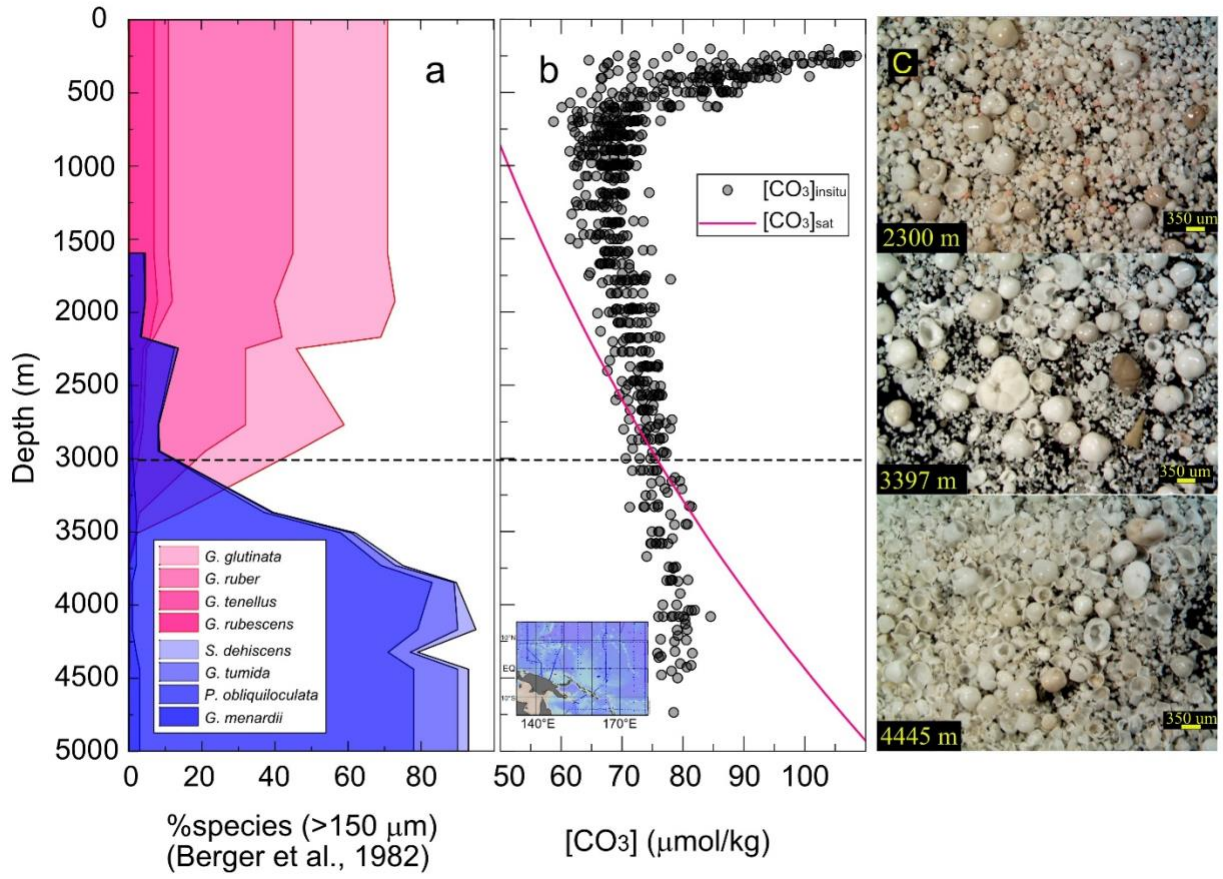

Figure S6. (a) changes in relative abundance of soluble (pink shaded) and dissolution resistant (blue shaded) over depth from Ontong-Java Plateau (Berger et al. 1982). (b) $[CO_3]_{sw}$ are calculated based on DIC and Alkalinity data from 155-180°E and 15°S-15°N (inlet) from GLODAP (Key et al. 2004). (c) light-microscope examination of the preservation of coretop planktonic foraminifera over depths. In the shallow-depth core (2300 m water depth), small pink *Globigerinoides ruber* shells are abundant in the foraminifera assemblage and decrease rapidly close to the depth of saturation horizon (panel A and B). At the 3397 mbsl core (~400m below the saturation horizon), the planktonic foraminifera assemblage becomes very different from above the saturation horizon, characterized by the enrichment of shells of more robust species such as *Pulleniatina obliquloculata* and *Globorotalia* spp.

Table S4: Sampling locations and water depths of Ontong-Java coretop

Sites	Latitudes & Longitudes	Water depth (km)
GGC-6	2˚14.81'S, 156˚59.85'E	1.6
GGC-8	2˚12.54'S, 156˚57.90'E	1.6
BC-33	0˚59.33'S, 157˚50.10'E	2.0
GGC-32	0˚59.33'S, 157˚50.10'E	2.0
GGC-15	0˚1.38'S, 158˚56.46'E	2.3
GGC-38	0˚0.35'S, 159˚22.02'E	2.4
GGC-41	0˚0.00'S, 159˚46.11'E	2.7
GGC-44	0˚0.04'S, 160˚39.11'E	3.1
BC-51	0˚0.47'S, 161˚0.20'E	3.4
GGC-48	0˚0.47'S, 161˚0.20'E	3.4
BC-53	0˚0.50'S, 161˚21.27'E	3.7
GGC-55	0˚0.87'S, 161˚46.43'E	4.0
BC-56	0˚0.06'S, 161˚47.39'E	4.0
GGC-71	0˚1.32'S, 162˚38.66'E	4.4
BC-74	0˚1.32'S, 162˚38.66'E	4.4

3.2 Planktonic foraminifera preservation from the western Equatorial Pacific since the Middle Miocene

Changes in the size index along the western Equatorial Pacific depth transect (Figure 3, main text) suggest that the preservation of planktonic foraminifera was particularly poor ~10 Ma but improved increasingly over time. This improvement is visible under the light microscope when >60 μm fraction is examined (Figure S7). In Site 803 (3.4 km), whole foraminiferal tests are nearly absent in the >60 μm fraction at ~10 Ma. In contrast, siliceous shells and heavily encrusted foraminiferal fragments are enriched, suggesting that most foraminifera tests have been dissolved, left only the recalcitrant components. In the same core, the numbers of whole foraminifera tests have clearly increased by ~6 Ma. More soluble species such as *Globigerinoides* spp. occur in the residues. In the Pleistocene, the preservation of foraminiferal

assemblages is nearly as good as at shallower depth Site 806 (2.5 km), show minor sign of dissolution.

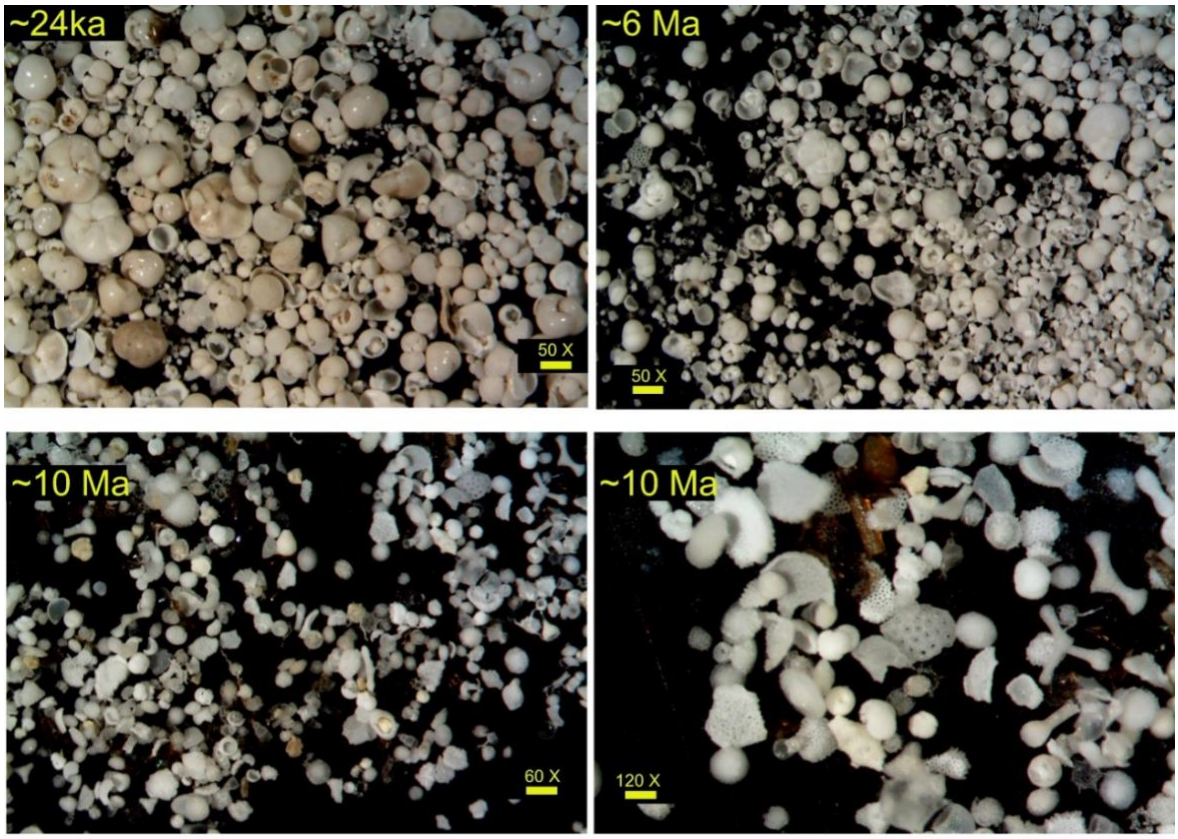

Figure S7. light microscope study of Site 803 (3.4 km) planktonic foraminifera in the >60 μm fraction.

3.3 CF-size index from locations outside of the equatorial Pacific

In addition to the equatorial Pacific, we also generated planktonic foraminifera size index from other sites in order to obtain a global coverage (Figure S8). Although the timing and pattern differ from site to site, all locations show improved preservation towards the Pleistocene.

673 In the equatorial Indian Ocean (Site 758), the preservation of foraminifera was generally good in
674 the Middle Miocene and the Pleistocene, but poor in the Late Miocene (5-10 Ma). In the
675 southwest Pacific (Site 590), the size index shows a two-step improvement in foraminifera
676 preservation at ~13-14 Ma and ~2.7 Ma, which are coincident with Mi3 glaciation and Northern
677 Hemisphere Glaciation, respectively. In the Caribbean Sea, size index was low until ~3 Ma.
678 Increased size index in the Pleistocene corresponds to increased MAR-foraminifera (Figure S1o),
679 suggesting improved preservation of planktonic foraminifera. In the equatorial Atlantic, size
680 index from Site 667 (3.5 km) and Site 928 (4 km) indicates that dissolution was particularly
681 strong in the Miocene. Most foraminifera became dissolved at/below 3.5 km. Foraminifer
682 preservation, however, significantly improved above the Miocene/Pliocene boundary. As a
683 result, the MAR-foraminifera from these two sites also increased after ~5 Ma (Fig. S1n and Fig.
684 S1q). In the South Atlantic, the size index from Site 1266 suggests that dissolution was strong at
685 ~3.5 km prior to 13 Ma. During ~13-14 Ma (~94-99 mcd), the foraminifer preservation
686 significantly improved. This change corresponds to an increase in B/Ca in benthic foraminifera,
687 which has been interpreted as an increase in $[CO_3]_{sw}$ by more than 60 μmol/kg (Kender et al.
688 2014).
689

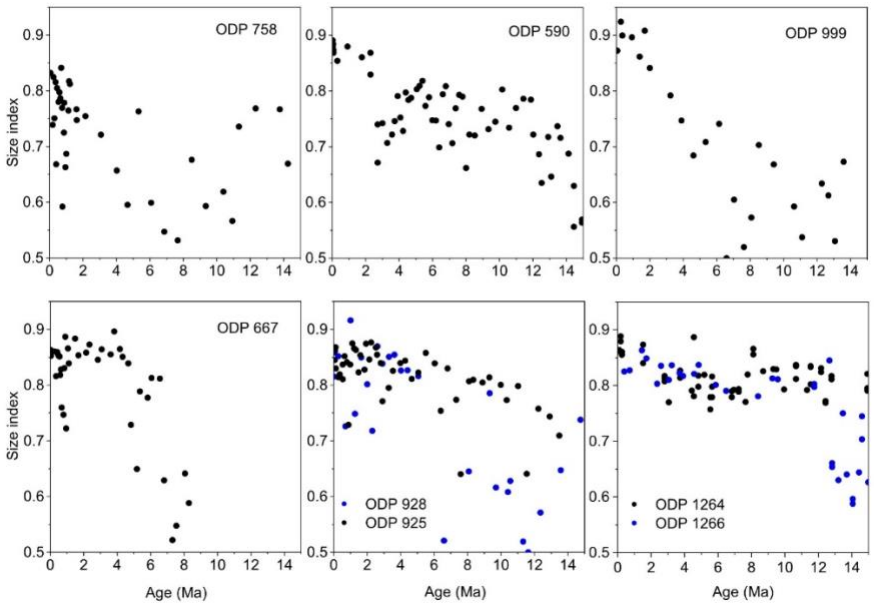

690

691 **Figure S8**. CF-Size index of planktonic foraminifera from the equatorial Indian Ocean (Site 758,
692 2.9 km), southwest Pacific (Site 590, 1.3 km), Caribbean Sea (Site 999, 2.8 km), equatorial
693 Atlantic (Site 667, 3.5 km, Site 925, 3.0 km, and Site 928, 4.0 km), and South Atlantic (Site
694 1264, 2.5 km, Site 1266, 3.8 km).

695

696 4. Potential biases in CF-size index

697 As a qualitative indicator of foraminifera dissolution, CF-size index, however, is not bias free.
698 For instance, the Miocene values of the size index in the shallowest Ontong Java Site 806 are as
699 low as the lowest values measured for the core top samples at ~4.5 km water depths (~0.7-0.8). If
700 we were to take the face values, then the CF-size index would suggest the seawater was as
701 corrosive at 2.5 km depth during the Miocene as at ~4.5 km during the Pleistocene. This would
702 imply a huge change in the [CO_3] of seawater over the last 15 Ma, and therefore raise the
703 concern that the CF-size index is somehow biased. We consider two potential sources of biases
704 here, including the evolution of planktonic foraminifera and burial diagenesis.

Although the late Neogene planktonic foraminifera show no major evolutionary radiation, the occurrences of certain lineages/species, particularly those thrive in tropic nutrientcline, have the potential to bias the temporal changes of CF-size index in Figure 3 (main text). These species include *Globorotalia menardii* complex (which also includes the *G. tumida* lineage) and *Pulleniatina obliquiloculata*. Species of *Globorotalia menardii* complex are characterized by the growth of robust keels throughout the test periphery and thick secondary crustal calcite towards the end of ontogeny. The other species, *Pulleniatina obliquiloculata*, similarly, have thick shiny veneer outer calcite that is resistant to dissolution (Johnstone et al. 2010). In general, these species are not the dominant components in foraminiferal fauna. But in severely dissolved Pleistocene samples, the concentration of *G. menardii*, *G. tumida*, and *P. obliquiloculata*. can increase significantly and increase the CF-size index.

In the western equatorial Pacific, *P. obliquiloculata* accounts for a sizable fraction (~5%) of the foraminifera assemblage in relative shallow coretop sediments (<3 km) (Figure S6). At 4.5 km, fragments of *P. obliquiloculata* can accounted for >60% of the foraminifera identified (Figure S6). Thus, CF-size index in Figure 3 (main text) may have "overestimated" foraminiferal preservation in Pleistocene samples relative to Miocene samples, particularly for deep sites such as Site 804. Relative to the Pleistocene, the absence of these species in Miocene samples may result in an underestimate of the preservation of the foraminifera.

726 On the other hand, these dissolution resistant thermocline species are limited to tropics and they
727 are absent/rare in Atlantic during glacial intervals in the late Pleistocene, so their influence on
728 size index outside the equatorial Indo-Pacific regions should be limited.
729
730 Burial diagenesis is another factor that should be considered. Increasing burial depth and
731 compaction can increase the fragmentation of foraminifera and potentially give rise to an artifact
732 of improved preservation over time. However, we argue that burial diagenesis should have only
733 played a minor role in the preservation of foraminifera. At Site 806, one of the thickest records
734 of this study, Miocene isotope data preserved SST and ^{13}C gradients among different species
735 (Holbourn et al. 2013, Nathan and Leckie 2009), suggesting that the preservation of planktonic
736 foraminifera is at least moderate. Besides, in contrast to the dry bulk density which shows a
737 monotonic increase with depth, CF-size index at Site 806 show better preservation in the Middle
738 Miocene (~13-14 Ma) than the late Middle Miocene (10-12 Ma) when sever dissolution occurred
739 during the carbonate crash in the equatorial Pacific. Because dry bulk density and CF-size index
740 do not covary, sedimentary compaction is unlikely a major concern for Middle Miocene samples
741
742 We do, however, observe changes in preservation due to post-burial diagenesis at Site 806 in the
743 Early Miocene. Recrystallization of foraminifera fragments due to diagenesis results in cemented
744 particles that are obvious in washed residues. Indeed, we purposely choose the Middle Miocene
745 as the cutoff point for this study because we concern that burial diagenesis in deeper sediments
746 can significantly bias our results.
747

5. Dissolution rates of foraminifera in the Miocene, Pleistocene and Holocene sediments

Here, we calculated the changes in MAR-foraminifera along the Ontong-Java depth transect. In the Middle Miocene (~13 Ma), MAR-foraminifera from Sites 806 and 807 are similar. In contrast, a large decrease in MAR-foraminifera occurs between Sites 807 and 803, suggesting that significant dissolution (>1 g/cm2 kyr) have occurred between 2.7 and 3.4 km. In the Pleistocene, MAR-foraminifera become very similar across the depth transect, indicating smaller dissolution rates of foraminifera (~0.2 g/cm2 kyr) over the depth range.

Using carbon-14 age from (Broecker et al. 1999a), MAR for Holocene samples can be calculated independently of the Pleistocene bio-magnetic-stratigraphy (Table S5). The calculation indicates dissolution rate of ~0.44 g/cm2 kyr over the depth range of 2.3-3.4 km, which is higher but of the same magnitude as our Pleistocene average.

Table S5. Estimates of Mass Accumulation Rates in Ontong-Java coretop samples

Core ID	Depth (km)	%$CaCO_3$	Sampling depth (cm)	MAR-bulk (g cm^{-2} kyr^{-1}) (Broecker et al. 1999a)	MAR-foraminifera (g cm^{-2} kyr^{-1})	MAR-coccolith (g cm^{-2} kyr^{-1})
GGC15	2.31	84	5-6	1.82 (based on BC-36)	0.98	0.56
BC-51	3.39	75	5-6	1.61	0.55	0.65
BC-53	3.68	81	4-5	1.26	0.30	0.72
BC-56	4.04	63	3-4	1.15	0.21	0.51
BC-74	4.44	68	5-6	0.76	0.12	0.38

6. Hypothetical scenarios of changes in carbonate production, dissolution and accumulation

In scenario 1 and 2 (Figure S9 a-b), carbonate production in the surface ocean is assumed to be constant. In scenario 1, the thickness of the transition zone is also assumed to be constant. The CCD, however, has deepened from the Miocene to the Pleistocene. This scenario, however, does not explain the observed large decreases in MARc in shallow sites in this study as well as in (Suchéras-Marx and Henderiks 2014). This Scenario is closest to the dissolution concept postulated/discussed in (Suchéras-Marx and Henderiks 2014). For instance, if accommodating changes in productivity, this scenario could also explain the "more dissolution" (shallower CCD), (much) more production and higher MAR during the Miocene. In scenario 2, the CCD remains relatively constant. The transition zone, however, is thinner in the Miocene than in the Pleistocene. In this case, we would expect less dissolution in the Miocene and therefore more burial, as indicated by the hypothetical curves of the $\%CaCO_3$. However, this scenario does not explain improved preservation in foraminifera and decreased dissolution (ΔMARc) along the depth transect over the last 15 Ma. In scenario 3, the transition zone is thicker in the Miocene and the dissolution is higher. The MARc, however, is also higher. Large decreases in MARc from the Miocene to the Pleistocene is not due to less dissolution but the decreased production.

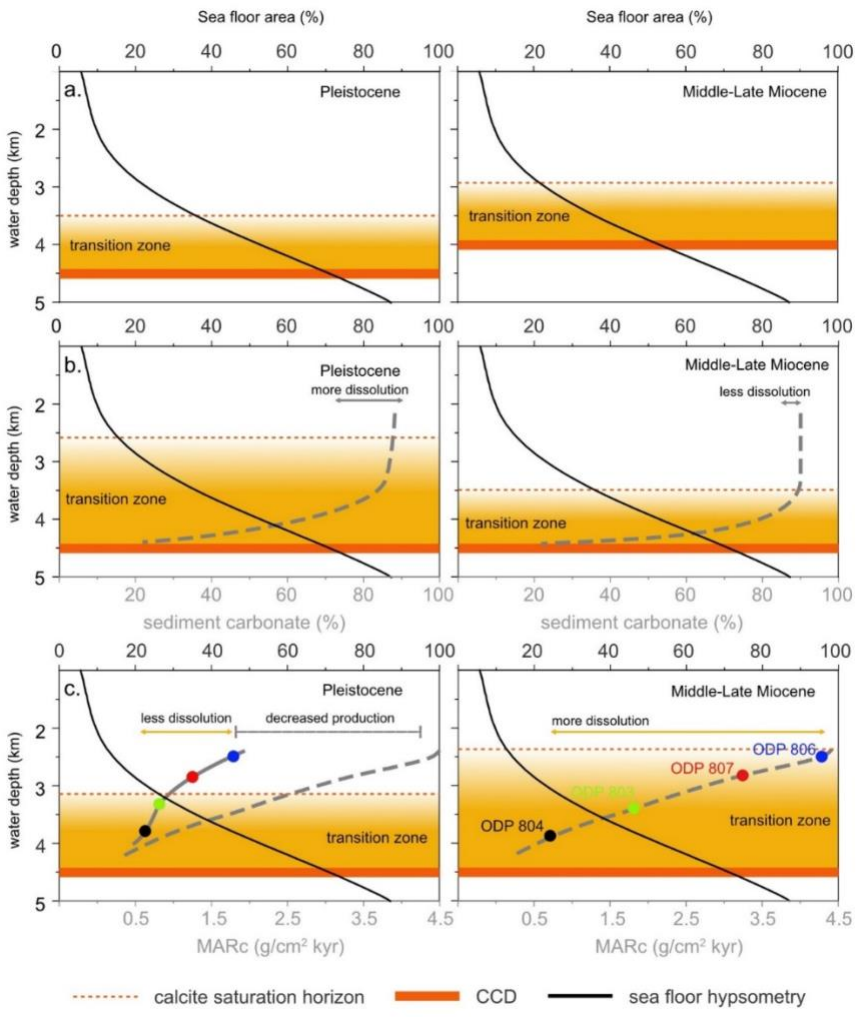

Figure S9. Three hypothetical scenarios of changes in carbonate production, dissolution and accumulation. Grey dash lines in (b) indicate hypothetical %$CaCO_3$ decrease with increasing water depth (undersaturation). Grey dash lines in (c) indicate changes in MARc that are constrained by the data from the western Equatorial Pacific.

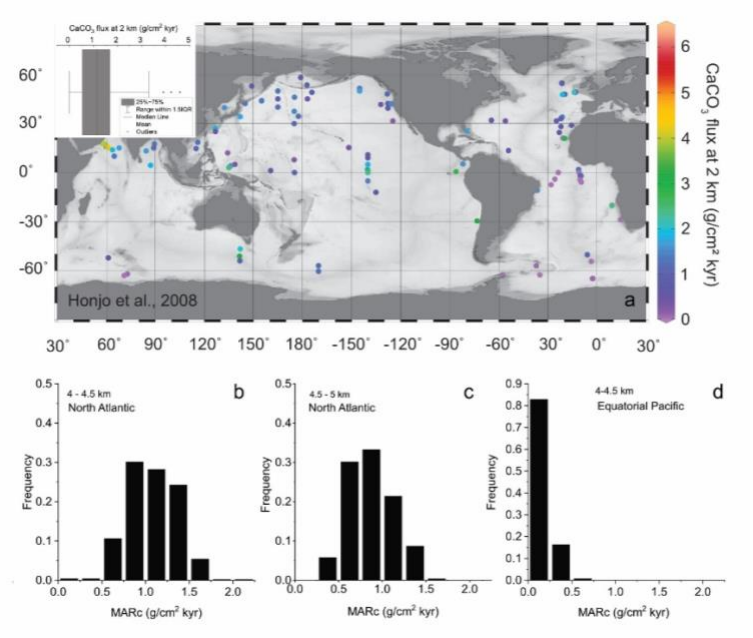

Figure S10. (a) Carbonate fluxes at 2 km based on sedimentary trap (Honjo et al. 2008) with a median value ~1.2 g/cm2 kyr (inset). (b-d) Carbonate burial fluxes estimates in the modern ocean based on model output (Dunne et al. 2012) which was optimized to fit the observed Holocene carbonate burial fluxes. Map generated by Ocean Data View (Schlitzer 2018). We select grids from interested depth intervals and collect MARc data from these grids and plot them in b-d respectively. The distribution of these MARc help constrains the increased carbonate burial fluxes due to a deeper Pleistocene CCD. For instance, in the North Atlantic, deepening of the CCD increased carbonate accumulation below 4 km. The magnitude of the increase is ~1.2 g/cm2 kyr between 4-5 km. In the equatorial Pacific, deepening CCD by ~500m in the Pleistocene had negligible effect on carbonate budget.

References

Beaufort, L., I. Probert, and N. Buchet. 2007. Effects of acidification and primary production on coccolith weight: Implications for carbonate transfer from the surface to the deep ocean. Geochemistry, Geophysics, Geosystems 8(8):doi.org/10.1029/2006GC001493

Berger, W. H., T. Bickert, H. Schmidt, and T. Wefer. 1993a. Quaternary oxygen isotope record of pelagic foraminifers; Site 806, Ontong Java Plateau. Proceedings of the Ocean Drilling Program; Ontong Java Plateau, covering Leg 130 of the cruises of the drilling vessel JOIDES Resolution, Apra Harbor, Guam, to Apra Harbor, Guam, Sites 805-807, 18 January-26 March 1990 130:381.

Berger, W. H., M. C. Bonneau, and F. L. Parker. 1982. Foraminifera on the Deep-Sea Floor - Lysocline and Dissolution Rate. Oceanologica Acta 5(2):249-258.

Berger, W. H., R. M. Leckie, T. R. Janecek, R. Stax, and T. Takayama. 1993b. Neogene carbonate sedimentation on Ontong Java Plateau; highlights and open questions. Proceedings of the Ocean Drilling Program; Ontong Java Plateau, covering Leg 130 of the cruises of the drilling vessel JOIDES Resolution, Apra Harbor, Guam, to Apra Harbor, Guam, Sites 805-807, 18 January-26 March 1990 130:711 %J Proceedings of the Ocean Drilling Program, Scientific Results.

Bickert, T., W. Curry, and G. Wefer. 1997. Late Pliocene to Holocene (2.6-0 Ma) western equatorial Atlantic deep-water circulation: inferences from benthic stable isotopes. Pp. 239-253. Proceedings of the Ocean Drilling Program. Scientific Results.

Bougault, H., S. C. Cande, J. C. Brannon, D. M. Christie, M. Clark, D. M. Curtis, N. Drake, D. J. Echols, I. A. Hill, M. J. Khan, W. G. Mills, R. Neuser, M. L. Rideout, and B. L. Weaver. 1985. Site 558. Initial reports of the Deep Sea Drilling Project; covering Leg 82 of the cruises of the Drilling Vessel Glomar Challenger; Ponta Delgada, Azores, to Balboa, Panama; September-November 1981 82:127.

Bralower, T. J., I. Premoli Silva, M. J. Malone, M. A. Arthur, K. Averyt, P. R. Bown, S. C. Brassell, J. E. T. Channell, L. J. Clarke, A. Dutton, J. W. Eleson, T. D. Frank, S. Gylesjo, H. Hancock, H. Kano, R. M. Leckie, K. M. Marsaglia, J. McGuire, K. T. Moe, M. R. Petrizzo, S. A. Robinson, U. Röhl, W. W. Sager, K. Takeda, D. Thomas, T. Williams, and J. C. Zachos. 2002. Site 1208. Proceedings of the Ocean Drilling Program, initial reports, extreme warmth in the Cretaceous and Paleogene; a depth transect on Shatsky Rise, Central Pacific; covering Leg 198 of the cruises of the drilling vessel JOIDES Resolution; Yokohama, Japan, to Honolulu, Hawaii; sites 1207-1214; 27 August-23 October 2001 198:93.

Broecker, W., and E. Clark. 2007. Is the magnitude of the carbonate ion decrease in the abyssal ocean over the last 8 kyr consistent with the 20 ppm rise in atmospheric CO2 content? Paleoceanography 22(1).

Broecker, W. S., and E. Clark. 1999. CaCO3 size distribution: A paleocarbonate ion proxy? Paleoceanography 14(5):596-604.

Broecker, W. S., E. Clark, D. C. McCorkle, I. Hajdas, and G. Bonani. 1999a. Core top 14C ages as a function of latitude and water depth on the Ontong-Java plateau. Paleoceanography 14(1):13-22.

Broecker, W. S., E. Clark, D. C. McCorkle, T.-H. Peng, I. Hajdas, and G. Bonani. 1999b. Evidence for a reduction in the carbonate ion content of the deep sea during the course of the Holocene. Paleoceanography 14(6):744-752.

Chiu, T. C., and W. S. Broecker. 2008. Toward better paleocarbonate ion reconstructions: New insights regarding the CaCO3 size index. Paleoceanography 23(2):doi.org/10.1029/2008PA001599

Curry, W. B., N. J. Shackleton, C. Richter, J. E. Backman, F. Bassinot, T. Bickert, W. P. Chaisson, J. L. Cullen, P. deMenocal, D. M. Dobson, L. Ewert, J. Grützner, T. K. Hagelberg, G. Hampt, S. E. Harris, T. D. Herbert, K. Moran, M. Murayama, D. W. Murray, P. N. Pearson, I. Raffi, D. A. Schneider, R. Tiedemann, J.-P. Valet, G. P. Weedon, H. Yasuda, and J. C. Zachos. 1995a. Site 925. Proceedings of the Ocean Drilling Program; initial reports; Ceara Rise; covering Leg 154 of the cruises of the drilling vessel JOIDES Resolution, Bridgetown, Barbados, to Bridgetown, Barbados, sites 925-929, 24 January-25 March 1994 154:55.

Curry, W. B., N. J. Shackleton, C. Richter, J. E. Backman, F. Bassinot, T. Bickert, W. P. Chaisson, J. L. Cullen, P. deMenocal, D. M. Dobson, L. Ewert, J. Grützner, T. K. Hagelberg, G. Hampt, S. E. Harris, T. D. Herbert, K. Moran, M. Murayama, D. W. Murray, P. N. Pearson, I. Raffi, D. A. Schneider, R. Tiedemann, J.-P. Valet, G. P. Weedon, H. Yasuda, and J. C. Zachos. 1995b. Site 928. Proceedings of the Ocean Drilling Program; initial reports; Ceara Rise; covering Leg 154 of the cruises of the drilling vessel JOIDES Resolution, Bridgetown, Barbados, to Bridgetown, Barbados, sites 925-929, 24 January-25 March 1994 154:281.

Dunne, J. P., B. Hales, and J. R. Toggweiler. 2012. Global calcite cycling constrained by sediment preservation controls. Global Biogeochemical Cycles 26(3):doi.org/10.1029/2010GB003935

Evans, H. F. 2006. Magnetic stratigraphy and environmental magnetism of oceanic sediments. Ph. D. University of Florida, Gainesville, FL, United States.

Exon, N. F., J. P. Kennett, M. J. Malone, H. Brinkhuis, G. C. H. Chaproniere, A. Ennyu, P. Fothergill, M. D. Fuller, M. Grauert, P. J. Hill, T. R. Janecek, D. C. Kelly, J. C. Latimer, S. Nees, U. S. Ninnemann, D. Nürnberg, S. F. Pekar, C. C. Pellaton, H. A. Pfuhl, C. M. Robert, K. L. M. Roessig, U. Röhl, S. A. Schellenberg, A. E. Shevenell, C. E. Stickley, N. Suzuki, Y. Touchard, W. Wei, and T. S. White. 2001. Site 1171. Proceedings of the Ocean Drilling Program, initial reports, the Tasmanian Gateway, Cenozoic climatic and oceanographic development; covering Leg 189 of the cruises of the drilling vessel JOIDES Resolution; Hobart, Tasmania, to Sydney, Australia; sites 1168-1172, 11 March-6 May 2000 189:176.

Farrell, J. W., D. W. Murray, V. S. McKenna, and A. C. Ravelo. 1995. Upper ocean temperature and nutrient contrasts inferred from Pleistocene planktonic foraminifer δ¹⁸O and δ¹³C in the eastern Equatorial Pacific. Proceedings of the Ocean Drilling Program; scientific results; eastern Equatorial Pacific, covering Leg 138 of the cruises of the drilling vessel JOIDES Resolution, Balboa, Panama, to San Diego, California, Sites 844-854, 1 May-4 July 1991 138:289.

Gersonde, R., D. A. Hodell, P. Blum, C. Andersson, W. E. N. Austin, K. Billups, J. E. T. Channell, C. D. Charles, B. Diekmann, G. M. Filippelli, J. A. Flores, A. T. Hewitt, W. R. Howard, M. Ikehara, T. R. Janecek, S. L. Kanfoush, A. E. S. Kemp, S. L. King, H. F. Kleiven, G. Kuhn, M. Marino, U. S. Ninnemann, S. O'Connell, J. D. Ortiz, J. S. Stoner, K. Sugiyama, D. A. Warnke, and U. Zielinski. 1999. Site 1088. Proceedings of the Ocean Drilling Program; initial reports; Southern Ocean paleoceanography; covering Leg 177 of the cruises of the drilling vessel JOIDES Resolution; Cape Town, South Africa, to Punta Arenas, Chile; sites 1088-1094; 9 December 1997-5 February 1998 177:66.

Hassenkam, T., A. Johnsson, K. Bechgaard, and S. L. Stipp. 2011. Tracking single coccolith dissolution with picogram resolution and implications for CO2 sequestration and ocean acidification. Proc Natl Acad Sci U S A 108(21):8571-6.

Haug, G. H., and R. Tiedemann. 1998. Effect of the formation of the Isthmus of Panama on Atlantic Ocean thermohaline circulation. Nature 393(6686):673-676.

Hodell, D. A., C. D. Charles, J. H. Curtis, P. G. Mortyn, U. S. Ninnemann, and K. A. Venz. 2003. Oxygen isotope stratigraphy of ODP Leg 177 sites 1088, 1089, 1090, 1093, and 1094. Proceedings of the Ocean Drilling Program, scientific results; Southern Ocean paleoceanography; covering Leg 177 of the cruises of the drilling vessel JOIDES Resolution; Cape Town, South Africa, to Punta Arenas, Chile; sites 1088-1094; 9 December 1997-5 February 1998 177:26.

Holbourn, A., W. Kuhnt, M. Frank, and B. A. Haley. 2013. Changes in Pacific Ocean circulation following the Miocene onset of permanent Antarctic ice cover. Earth and Planetary Science Letters 365:38-50.

Honjo, S., J. Dymond, R. Collier, and S. J. Manganini. 1995. Export production of particles to the interior of the equatorial Pacific Ocean during the 1992 EqPac experiment. Deep Sea Research Part II: Topical Studies in Oceanography 42(2-3):831-870.

Honjo, S., and J. Erez. 1978. Dissolution rates of calcium carbonate in the deep ocean; an in-situ experiment in the North Atlantic Ocean. Earth and Planetary Science Letters 40(2):287-300.

Honjo, S., S. J. Manganini, R. A. Krishfield, and R. Francois. 2008. Particulate organic carbon fluxes to the ocean interior and factors controlling the biological pump: A synthesis of global sediment trap programs since 1983. Progress in Oceanography 76(3):217-285.

Jansen, E., M. E. Raymo, P. Blum, E. S. Andersen, W. E. N. Austin, K.-H. Baumann, V. Bout-Roumazeilles, S. J. Carter, J. E. T. Channell, J. L. Cullen, B. Flower, S. Higgins, D. A. Hodell, J. A. Hood, S. M. Hyun, M. Ikehara, T. King, R. Larter, B. Lehman, S. Locker, K. McIntyre, J. McManus, L. B. Meng, S. O'Connell, J. D. Ortiz, F. R. Rack, A. Solheim, and W. Wei. 1996. Site 982. Proceedings of the Ocean Drilling Program; initial reports; North Atlantic-Arctic gateways II; covering Leg 162 of the cruises of the drilling vessel JOIDES Resolution, Edinburgh, United Kingdom, to Málaga, Spain, Sites 980-987, 7 July-2 September 1995 162:91.

Johnstone, H. J. H., M. Schulz, S. Barker, and H. Elderfield. 2010. Inside story: An X-ray computed tomography method for assessing dissolution in the tests of planktonic foraminifera. Marine Micropaleontology 77(1-2):58-70.

Keir, R., and W. Berger. 1985. Late Holocene carbonate dissolution in the equatorial Pacific: reef growth or neoglaciation? in The Carbon Cycle and Atmospheric CO2: Natural Variations Archean to Present. vol. 32, edited by E.T. Sundquist and W.S. Broecker, pp. 208-219, AGU, Washington, D.C., 1985.

Kender, S., J. Yu, and V. L. Peck. 2014. Deep ocean carbonate ion increase during mid Miocene CO 2 decline. Scientific Reports 4:doi.org/10.1038/srep04187.

Kennett, J. P., C. C. von der Borch, P. A. Baker, C. E. Barton, A. Boersma, J. P. Caulet, W. C. Dudley, Jr., J. V. Gardner, D. G. Jenkins, W. H. Lohman, E. Martini, R. B. Merrill, R. H. Morin, C. S. Nelson, C. Robert, M. S. Srinivasan, R. Stein, and A. Takeuchi. 1986a. Site 588; Lord Howe Rise, 26°S. Initial reports of the Deep Sea Drilling Project covering Leg 90 of the cruises of the drilling vessel Glomar Challenger; Noumea, New Caledonia, to Wellington, New Zealand, December 1982-January 1983; Part 1 90:139.

Kennett, J. P., C. C. von der Borch, P. A. Baker, C. E. Barton, A. Boersma, J. P. Caulet, W. C. Dudley, Jr., J. V. Gardner, D. G. Jenkins, W. H. Lohman, E. Martini, R. B. Merrill, R. H. Morin, C. S. Nelson, C. Robert, M. S. Srinivasan, R. Stein, and A. Takeuchi. 1986b. Site 590; Lord Howe Rise, 31°S. Initial reports of the Deep Sea Drilling Project covering Leg 90 of the cruises of the drilling vessel Glomar Challenger; Noumea, New Caledonia, to Wellington, New Zealand, December 1982-January 1983; Part 1 90:263.

Kennett, J. P., C. C. von der Borch, P. A. Baker, C. E. Barton, A. Boersma, J. P. Caulet, W. C. Dudley, Jr., J. V. Gardner, D. G. Jenkins, W. H. Lohman, E. Martini, R. B. Merrill, R. H. Morin, C. S. Nelson, C. Robert, M. S. Srinivasan, R. Stein, and A. Takeuchi. 1986c. Site 593; Challenger Plateau. Initial reports of the Deep Sea Drilling Project covering Leg 90 of the cruises of the drilling vessel Glomar Challenger; Noumea, New Caledonia, to Wellington, New Zealand, December 1982-January 1983; Part 1 90:551.

Key, R. M., A. Kozyr, C. L. Sabine, K. Lee, R. Wanninkhof, J. L. Bullister, R. A. Feely, F. J. Millero, C. Mordy, and T. H. Peng. 2004. A global ocean carbon climatology: Results from Global Data Analysis Project (GLODAP). Global Biogeochemical Cycles 18(4):doi.org/10.1029/2004GB002247

Kroenke, L. W., W. H. Berger, T. R. Janecek, J. Backman, F. Bassinot, R. M. Corfield, M. L. Delaney, R. A. Hagen, E. Jansen, L. A. Krisek, C. Lange, R. M. Leckie, I. L. Lind, M. W. Lyle, J. J. Mahoney, J. C. Marsters, L. A. Mayer, D. C. Mosher, R. Musgrave, M. L. Prentice, J. M. Resig, H. Schmidt, R. Stax, M. Storey, K. Takahashi, T. Takayama, J. A. Tarduno, R. H. Wilkens, and G. Wu. 1991a. Site 806. Proceedings of the Ocean Drilling Program, Ontong Java Plateau, covering Leg 130 of the cruises of the drilling vessel JOIDES Resolution, Apra Harbor, Guam, to Apra Harbor, Guam, sites 803-807, 18 January 1990-26 March 1990 130:291.

Kroenke, L. W., W. H. Berger, T. R. Janecek, J. Backman, F. Bassinot, R. M. Corfield, M. L. Delaney, R. A. Hagen, E. Jansen, L. A. Krissek, C. Lange, R. M. Leckie, I. L. Lind, M. W. Lyle, J. J. Mahoney, J. C. Marsters, L. A. Mayer, D. C. Mosher, R. Musgrave, M. L. Prentice, J. M. Resig,

H. Schmidt, R. Stax, M. Storey, K. Takahashi, T. Takayama, J. A. Tarduno, R. H. Wilkens, and G. Wu. 1991b. Site 803. Proceedings of the Ocean Drilling Program, Ontong Java Plateau, covering Leg 130 of the cruises of the drilling vessel JOIDES Resolution, Apra Harbor, Guam, to Apra Harbor, Guam, sites 803-807, 18 January 1990-26 March 1990 130:101.

Kroenke, L. W., W. H. Berger, T. R. Janecek, J. Backman, F. Bassinot, R. M. Corfield, M. L. Delaney, R. A. Hagen, E. Jansen, L. A. Krissek, C. Lange, R. M. Leckie, I. L. Lind, M. W. Lyle, J. J. Mahoney, J. C. Marsters, L. A. Mayer, D. C. Mosher, R. Musgrave, M. L. Prentice, J. M. Resig, H. Schmidt, R. Stax, M. Storey, K. Takahashi, T. Takayama, J. A. Tarduno, R. H. Wilkens, and G. Wu. 1991c. Site 804. Proceedings of the Ocean Drilling Program, Ontong Java Plateau, covering Leg 130 of the cruises of the drilling vessel JOIDES Resolution, Apra Harbor, Guam, to Apra Harbor, Guam, sites 803-807, 18 January 1990-26 March 1990 130:177.

Kroenke, L. W., W. H. Berger, T. R. Janecek, J. Backman, F. Bassinot, R. M. Corfield, M. L. Delaney, R. A. Hagen, E. Jansen, L. A. Krissek, C. Lange, R. M. Leckie, I. L. Lind, M. W. Lyle, J. J. Mahoney, J. C. Marsters, L. A. Mayer, D. C. Mosher, R. Musgrave, M. L. Prentice, J. M. Resig, H. Schmidt, R. Stax, M. Storey, K. Takahashi, T. Takayama, J. A. Tarduno, R. H. Wilkens, and G. Wu. 1991d. Site 807. Proceedings of the Ocean Drilling Program, Ontong Java Plateau, covering Leg 130 of the cruises of the drilling vessel JOIDES Resolution, Apra Harbor, Guam, to Apra Harbor, Guam, sites 803-807, 18 January 1990-26 March 1990 130:369.

Lawrence, K. T., I. Bailey, and M. E. Raymo. 2013. Re-evaluation of the age model for North Atlantic Ocean Site 982 – arguments for a return to the original chronology. Climate of the Past 9(5):2391-2397.

Lisiecki, L. E., and M. E. Raymo. 2005. A Pliocene-Pleistocene stack of 57 globally disturbed benthic δ¹⁸O records. Paleoceanography 20(1):doi: 10.1029/2004PA001071.

Littke, R., J. Rullkötter, and R. G. Schaefer. 1991. Organic and carbonate carbon accumulation on Broken Ridge and Ninetyeast Ridge, central Indian Ocean. Proceedings of the Ocean Drilling Program, Broken Ridge and Ninetyeast Ridge; covering Leg 121 of the cruises of the drilling vessel JOIDES Resolution, Fremantle, Australia, to Port of Singapore, Singapore, sites 752-758, 30 April to 28 June 1988 121:467.

Lohman, W. H. 1986. Calcareous nannoplankton biostratigraphy of the southern Coral Sea, Tasman Sea, and southwestern Pacific Ocean, Deep Sea Drilling Project Leg 90; Neogene and Quaternary. Initial reports of the Deep Sea Drilling Project covering Leg 90 of the cruises of the drilling vessel Glomar Challenger, Noumea, New Caledonia, to Wellington, New Zealand, December 1982-January 1983 90:763.

Lopes, C., M. Kucera, and A. C. Mix. 2015. Climate change decouples oceanic primary and export productivity and organic carbon burial. Proceedings of the National Academy of Sciences 112(2):332-335.

Lyle, M. 2003. Neogene carbonate burial in the Pacific Ocean. Paleoceanography 18(3):doi:10.1029/2002PA000777.

Mayer, L. A., N. G. Pisias, T. R. Janecek, J. G. Baldauf, S. F. Bloomer, K. A. Dadey, K.-C. Emeis, J. Farrell, J. A. Flores, E. M. Galimov, T. K. Hagelberg, P. Holler, S. A. Hovan, M. Iwai, A. E. S. Kemp, D. C. Kim, G. Klinkhammer, M. Leinen, S. Levi, M. A. Levitan, M. W. Lyle, A. K. MacKillop, L. M. Meynadier, A. C. Mix, T. C. Moore, Jr., I. Raffi, C. Ravelo, D. Schneider, N. J. Shackleton, J.-P. Valet, and E. Vincent. 1991a. Site 846. Proceedings of the Ocean Drilling Program; Initial reports; Part 1, Eastern Equatorial Pacific; covering Leg 138 of the cruises of the drilling vessel JOIDES Resolution, Balboa, Panama, to San Diego, California, sites 844-854, 6 May 1991-5 July 1991 138:265.

Mayer, L. A., N. G. Pisias, T. R. Janecek, J. G. Baldauf, S. F. Bloomer, K. A. Dadey, K.-C. Emeis, J. Farrell, J. A. Flores, E. M. Galimov, T. K. Hagelberg, P. Holler, S. A. Hovan, M. Iwai, A. E. S. Kemp, D. C. Kim, G. Klinkhammer, M. Leinen, S. Levi, M. A. Levitan, M. W. Lyle, A. K. MacKillop, L. M. Meynadier, A. C. Mix, T. C. Moore, Jr., I. Raffi, C. Ravelo, D. Schneider, N. J. Shackleton, J.-P. Valet, and E. Vincent. 1991b. Site 847. Proceedings of the Ocean Drilling

Program; Initial reports; Part 1, Eastern Equatorial Pacific; covering Leg 138 of the cruises of the drilling vessel JOIDES Resolution, Balboa, Panama, to San Diego, California, sites 844-854, 6 May 1991-5 July 1991 138:335.

Mayer, L. A., N. G. Pisias, T. R. Janecek, J. G. Baldauf, S. F. Bloomer, K. A. Dadey, K.-C. Emeis, J. Farrell, J. A. Flores, E. M. Galimov, T. K. Hagelberg, P. Holler, S. A. Hovan, M. Iwai, A. E. S. Kemp, D. C. Kim, G. Klinkhammer, M. Leinen, S. Levi, M. A. Levitan, M. W. Lyle, A. K. MacKillop, L. M. Meynadier, A. C. Mix, T. C. Moore, Jr., I. Raffi, C. Ravelo, D. Schneider, N. J. Shackleton, J.-P. Valet, and E. Vincent. 1991c. Site 849. Proceedings of the Ocean Drilling Program; Initial reports; Part 1, Eastern Equatorial Pacific; covering Leg 138 of the cruises of the drilling vessel JOIDES Resolution, Balboa, Panama, to San Diego, California, sites 844-854, 6 May 1991-5 July 1991 138:735.

Mayer, L. A., N. G. Pisias, T. R. Janecek, J. G. Baldauf, S. F. Bloomer, K. A. Dadey, K.-C. Emeis, J. Farrell, J. A. Flores, E. M. Galimov, T. K. Hagelberg, P. Holler, S. A. Hovan, M. Iwai, A. E. S. Kemp, D. C. Kim, G. Klinkhammer, M. Leinen, S. Levi, M. A. Levitan, M. W. Lyle, A. K. MacKillop, L. M. Meynadier, A. C. Mix, T. C. Moore, Jr., I. Raffi, C. Ravelo, D. Schneider, N. J. Shackleton, J.-P. Valet, and E. Vincent. 1991d. Site 850. Proceedings of the Ocean Drilling Program; Initial reports; Part 1, Eastern Equatorial Pacific; covering Leg 138 of the cruises of the drilling vessel JOIDES Resolution, Balboa, Panama, to San Diego, California, sites 844-854, 6 May 1991-5 July 1991 138:809.

Mix, A. C., N. G. Pisias, W. Rugh, J. Wilson, A. Morey, and T. K. Hagelberg. 1995. Benthic foraminifer stable isotope record from Site 849 (0-5 Ma); local and global climate changes. Proceedings of the Ocean Drilling Program; scientific results; eastern Equatorial Pacific, covering Leg 138 of the cruises of the drilling vessel JOIDES Resolution, Balboa, Panama, to San Diego, California, Sites 844-854, 1 May-4 July 1991 138:371.

Mix, A. C., R. Tiedemann, P. Blum, F. F. Abrantes, H. Benway, I. Cacho-Lascorz, M.-T. Chen, M. L. Delaney, J.-A. Flores, L. Giosan, A. E. Holbourn, T. Irino, M. Iwai, L. H. Joseph, H. F. Kleiven, F. Lamy, P. Martinez, J. F. McManus, U. S. Ninnemann, N. G. Pisias, R. S. Robinson, J. S. Stoner, A. Sturm, M. W. Wara, and W. Wei. 2003. Site 1237. Proceedings of the Ocean Drilling Program, initial reports, Southeast Pacific paleoceanographic transects; covering Leg 202 of the cruises of the drilling vessel JOIDES Resolution; Valparaiso, Chile, to Balboa, Panama; sites 1232-1242, 29 March-30 May 2002 202:107.

Nathan, S. A., and R. M. Leckie. 2009. Early history of the Western Pacific Warm Pool during the middle to late Miocene (~13.2–5.8 Ma): Role of sea-level change and implications for equatorial circulation. Palaeogeography, Palaeoclimatology, Palaeoecology 274(3-4):140-159.

Pälike, H., M. W. Lyle, H. Nishi, I. Raffi, A. Ridgwell, K. Gamage, A. Klaus, G. Acton, L. Anderson, and J. Backman. 2012. A Cenozoic record of the equatorial Pacific carbonate compensation depth. Nature 488(7413):609.

Pälike, H., Nishi, H., Lyle, M., Raffi, I., Gamage, K., Klaus, A., and the Expedition 320/321 Scientists. 2010. Expedition 320/321summary. Proc. IODP, 320/321: Tokyo (Integrated Ocean Drilling Program Management International, Inc.). 320/321.

Peirce, J. W., J. K. Weissel, E. Taylor, J. Dehn, N. Driscoll, J. Farrell, E. Fourtanier, F. A. Frey, P. D. Gamson, J. S. Gee, I. L. Gibson, T. R. Janecek, C. Klootwijk, J. R. Lawrence, R. Littke, J. S. Newman, R. Nomura, R. M. Owen, J. J. Pospichal, D. K. Rea, P. Resiwati, A. D. Saunders, J. Smit, G. M. Smith, K. Tamaki, D. Weis, and C. Wilkinson. 1989a. Site 754. Broken Ridge and Ninetyeast Ridge; covering Leg 121 of the cruises of the drilling vessel JOIDES Resolution, Fremantle, Australia, to Port of Singapore, sites 752-758, 30 April to 28 June 1988 121:191.

Peirce, J. W., J. K. Weissel, E. Taylor, J. Dehn, N. Driscoll, J. Farrell, E. Fourtanier, F. A. Frey, P. D. Gamson, J. S. Gee, I. L. Gibson, T. R. Janecek, C. Klootwijk, J. R. Lawrence, R. Littke, J. S. Newman, R. Nomura, R. M. Owen, J. J. Pospichal, D. K. Rea, P. Resiwati, A. D. Saunders, J. Smit, G. M. Smith, K. Tamaki, D. Weis, and C. Wilkinson. 1989b. Site 758. Broken Ridge and

Ninetyeast Ridge; covering Leg 121 of the cruises of the drilling vessel JOIDES Resolution, Fremantle, Australia, to Port of Singapore, sites 752-758, 30 April to 28 June 1988 121:359.
Peterson, L., and J. Backman. 1990. Late Cenozoic carbonate accumulation and the history of the carbonate compensation depth in the western equatorial Indian Ocean. Proc., scientific results, ODP, Leg 115, Mascarene Plateau. ODP, Texas A&M University, College Station; UK distributors, IPOD Committee, NERC, Swindon.
Roth, P. H., and W. Berger. 1975. Distribution and dissolution of coccoliths in the south and central Pacific. CushmanFoundation for Foraminiferal Research Special Publication 13:87-113.
Ruddiman, W., M. Sarnthein, J. Baldauf, J. Backman, J. Bloemendal, W. Curry, P. Farrimond, J. C. Faugeres, T. Janacek, Y. Katsura, H. Manivit, J. Mazzullo, J. Mienert, E. Pokras, M. Raymo, P. Schultheiss, R. Stein, L. Tauxe, J.-P. Valet, P. Weaver, and H. Yasuda. 1988. Site 667. Proceedings of the Ocean Drilling Program, eastern tropical Atlantic, covering Leg 108 of the cruises of the drilling vessel JOIDES Resolution, Marseille, France, to Dakar, Senegal, sites 657-668, 18 February 1986-17 April 1986 108:833.
Ruddiman, W. F., R. B. Kidd, J. G. Baldauf, B. M. Clement, J. F. Dolan, M. R. Eggers, P. R. Hill, L. D. Keigwin, Jr., M. Mitchell, I. Philipps, F. Robinson, S. A. Salehipour, T. Takayama, E. Thomas, G. Unsold, and P. P. E. Weaver. 1987a. Site 607. Initial reports of the Deep Sea Drilling Project covering Leg 94 of the cruises of the drilling vessel Glomar Challenger, Norfolk, Virginia, to St. John's, Newfoundland, June-August 1983 94(1):75.
Ruddiman, W. F., R. B. Kidd, J. G. Baldauf, B. M. Clement, J. F. Dolan, M. R. Eggers, P. R. Hill, L. D. Keigwin, Jr., M. Mitchell, I. Philipps, F. Robinson, S. A. Salehipour, T. Takayama, E. Thomas, G. Unsold, and P. P. E. Weaver. 1987b. Site 608. Initial reports of the Deep Sea Drilling Project covering Leg 94 of the cruises of the drilling vessel Glomar Challenger, Norfolk, Virginia, to St. John's, Newfoundland, June-August 1983 94(1):149.
Schlitzer, R. 2018. Ocean Data View, odv.awi.de.
Sexton, P. F., and S. Barker. 2012. Onset of 'Pacific-style' deep-sea sedimentary carbonate cycles at the mid-Pleistocene transition. Earth and Planetary Science Letters 321-322:81-94.
Shackleton, N. J., S. Crowhurst, T. Hagelberg, N. G. Pisias, and D. A. Schneider. 1995. A new late Neogene time scale; application to Leg 138 sites. Proceedings of the Ocean Drilling Program; scientific results; eastern Equatorial Pacific, covering Leg 138 of the cruises of the drilling vessel JOIDES Resolution, Balboa, Panama, to San Diego, California, Sites 844-854, 1 May-4 July 1991 138:73.
Sigurdsson, H., R. M. Leckie, G. D. Acton, L. J. Abrams, T. J. Bralower, S. N. Carey, W. P. Chaisson, P. Cotillon, A. D. Cunningham, S. L. D'Hondt, A. W. Droxler, B. Galbrun, J. Gonzalez, G. Haug, K. Kameo, J. King, I. L. Lind, V. Louvel, T. W. Lyons, R. W. Murray, M. Mutti, G. Myers, R. B. Pearce, D. G. Pearson, L. C. Peterson, and U. Röhl. 1997. Site 999. Proceedings of the Ocean Drilling Program; Initial reports; Caribbean ocean history and the Cretaceous/Tertiary boundary event; covering Leg 165 of the cruises of the Drilling Vessel JOIDES Resolution, Miami, Florida, to San Juan, Puerto Rico, sites 998-1002, 19 December 1995-17 February 1996 165:131.
Suchéras-Marx, B., and J. Henderiks. 2014. Downsizing the pelagic carbonate factory: Impacts of calcareous nannoplankton evolution on carbonate burial over the past 17 million years. Global and Planetary Change 123:97-109.
Takayama, T. 1993. Notes on Neogene calcareous nannofossil biostratigraphy of the Ontong Java Plateau and size variations of Reticulofenestra coccoliths. Pp. 179-230. Proc. ODP, Sci. Res. Ocean Drilling Program.
Wilkens, R., T. Westerhold, A. J. Drury, M. Lyle, T. Gorgas, and J. Tian. 2017. Revisiting the Ceara Rise, equatorial Atlantic Ocean: isotope stratigraphy of ODP Leg 154. Climate of the Past 13:779-793.
Zachos, J., D. Kroon, P. Blum, J. Bowles, P. Gaillot, T. Hasegawa, and E. Hathorne. 2004a. Proceedings of the Ocean Drilling Program, Initial Reports, Volume 208.

Zachos, J. C., D. Kroon, P. Blum, J. Bowles, P. Gaillot, T. Hasegawa, E. C. Hathorne, D. A. Hodell, D. C. Kelly, J.-H. Jung, S. M. Keller, Y. S. Lee, D. C. Leuschner, L. Zhifei, K. C. Lohmann, L. Lourens, S. Monechi, M. J. Nicolo, I. Raffi, C. Riesselman, U. Röhl, S. A. Schellenberg, D. Schmidt, A. Sluijs, D. J. Thomas, E. Thomas, and H. Vallius. 2004b. Site 1264. Proceedings of the Ocean Drilling Program; initial reports; early Cenozoic extreme climates; the Walvis Ridge Transect; covering Leg 208 of the cruises of the drilling vessel JOIDES Resolution; Rio de Janeiro, Brazil, to Rio de Janeiro, Brazil; sites 1262-1267, 6 March-6 May 2003 208:73.

Zachos, J. C., D. Kroon, P. Blum, J. Bowles, P. Gaillot, T. Hasegawa, E. C. Hathorne, D. A. Hodell, D. C. Kelly, J.-H. Jung, S. M. Keller, Y. S. Lee, D. C. Leuschner, L. Zhifei, K. C. Lohmann, L. Lourens, S. Monechi, M. J. Nicolo, I. Raffi, C. Riesselman, U. Röhl, S. A. Schellenberg, D. Schmidt, A. Sluijs, D. J. Thomas, E. Thomas, and H. Vallius. 2004c. Site 1266. Proceedings of the Ocean Drilling Program; initial reports; early Cenozoic extreme climates; the Walvis Ridge Transect; covering Leg 208 of the cruises of the drilling vessel JOIDES Resolution; Rio de Janeiro, Brazil, to Rio de Janeiro, Brazil; sites 1262-1267, 6 March-6 May 2003 208:79.